Blocking Top-down awareness of Kanizsa Figures: An ERP Investigation into Bottom-up Processing of Illusory Contours

by

Allan Campopiano

Behavioral and Cognitive Neuroscience

Submission in partial fulfillment

of the requirements for the degree of

Master of Arts

Faculty of Social Sciences, Brock University

St. Catharines, Ontario

Abstract

Neural models of the processing of illusory contour (ICs) diverge from one another in terms of their emphasis on bottom-up versus top-down constituents. The current study uses a dichoptic fusion paradigm to block top-down awareness of ICs in order to examine possible bottom-up effects. Group results indicate that the N170 ERP component is particularly sensitive to ICs at central occipital sites when top-down awareness of the stimulus is permitted. Furthermore, single-subject statistics reveal that the IC N170 ERP effect is highly variable across individuals in terms of timing and topographical spread. The results suggest that the ubiquitous N170 effect to ICs found in the literature depends, at least in part, on participants' awareness of the stimulus. Therefore a strong bottom-up model of IC processing at the time of the N170 is unlikely.

Table of Contents

List of Figures

List of Abbreviations

ERP Event-related Potential

EEG Electroencephalography

MEG Magnetoencephalography

fMRI FunctionalMagneticResonanceImaging

BOLD Blood Oxygen Level Dependent

LOC Lateral Occipital Complex

LO Lateral Occipital Area

CoS Collateral sulcus

pFs Posterior fusiform gyrus

IC Illusory Contour

CI Confidence Interval

AS Aligned Same Condition

AO Aligned Opposite Condition

MS Misaligned Same Condition

MO Misaligned Opposite Condition

Introduction

One essential function of the visual system (among many) is to segregate a scene into coherent objects by using contrast and luminance cues to define object contours (Seghier & Vuilleumier, 2006), yet object contours may be perceived in the absence of any real object. These so-called illusory contours (ICs) were first mentioned by Schumann (1900); however, it was Kanizsa (1955) who provided the best-known examples of ICs as well as an explanation for the phenomenon. Based on Gestalt concepts, Kanizsa claimed that ICs arise from the perceptual completion of fragmented objects, leading to the simplest explanation of the visual stimulus. Although Kanizsa's initial theory was found to be insufficient (even by himself) (Kanizsa, 1975), his seminal paper inspired much scientific debate on ICs that still continues.

Neural regions and time-courses relating to IC processing have been identified, with some degree of consistency across a variety of methodologies (optical imaging, fMRI, EEG, MEG, PET, and single-unit recordings). However, extant models diverge from one another in their emphasis on the role of bottom-up and top-down factors during the perception of ICs. Bottom-up and top-down have been loosely defined in many ways. Respectively they can be synonymous with sensory-input driven and conceptually driven, physiological and cognitive, peripheral and central, or feed-forward and feedback neural architectures (Pritchard & Warm 1983; Murray, 2013). The current experiment simply refers to bottom-up as a largely automatic process whereas top-down involves a greater role for awareness, these being the most commonly understood overarching features of the terms (Pritchard & Warm, 1983).

Whether or not ICs are interpreted as primarily bottom-up or top-down stems partly from the methodology being used (Seghier & Vuilleumier, 2006; Murray & Herrmann, 2013). Low-

level accounts tend to focus on V1 and V2 areas whereas high-level accounts emphasize the role of the lateral occipital complex (LOC) (see Figure 1). The hierarchical anatomical connections in the primate visual system support the distinction between low-level (V1/V2) and high-level regions (LOC).[1] Further support of this distinction comes from the difference in receptive field properties of these visual regions. V1/V2 are arranged retinotopically and contain relatively small receptive fields. On the other hand, higher-tier cortices (e.g., LOC) are position-, cue-, and size-invariant and possess large receptive fields (Murray, 2013; Felleman & Van Essen, 1991).[2]

[1] Based on structural connectivity studies, anterior portions of the LOC (near VOT [ventral occipitotemporal]) feed back to V2 areas, although not to V1 or V3 areas. Posterior portions (near the fusiform gyrus), however, do not feed back to V1 or V2 areas directly (Felleman & Van Essen, 1991).

[2] The LOC begins at the lateral occipital sulcus and extends anteriorly and ventrally into posterior temporal visual areas around the fusiform gyrus (Grill-Spector, Kourtzi, & Kanwisher, 2001).

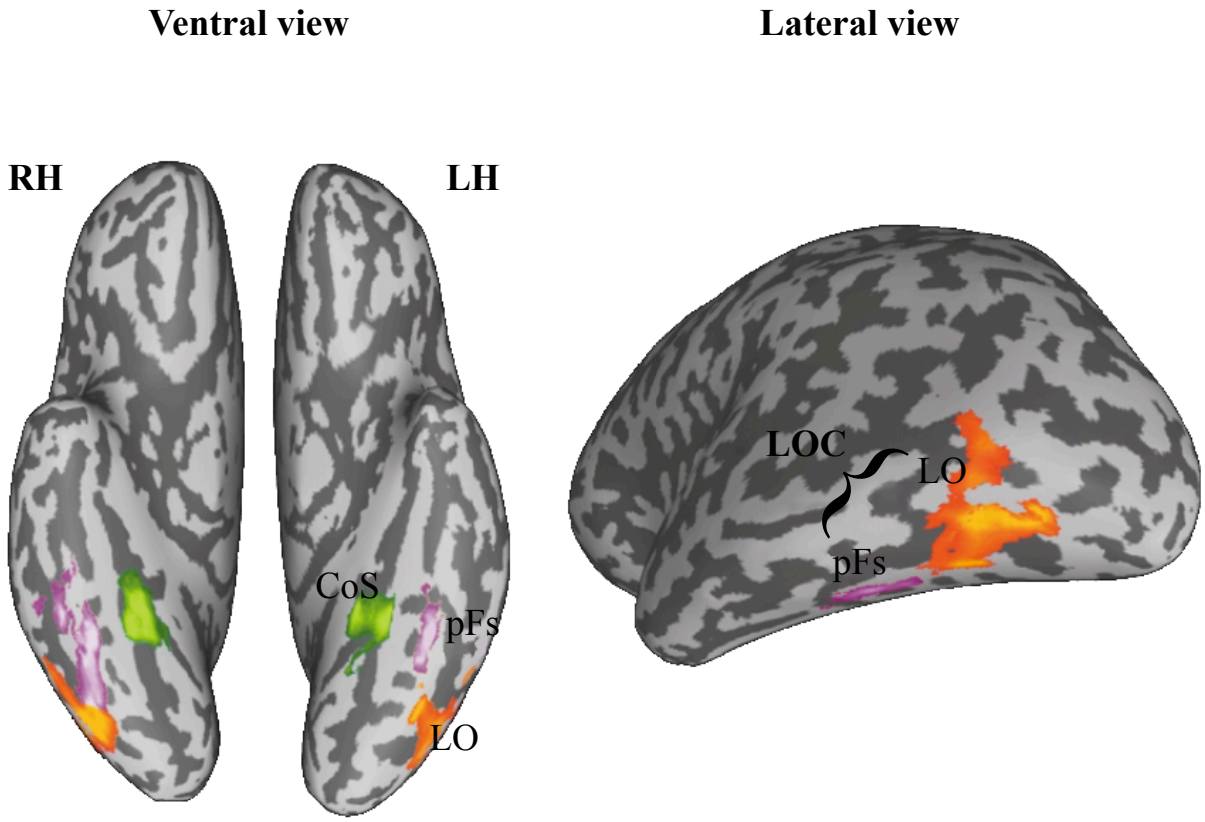

Figure 1. Regions of the lateral occipital complex (LOC) are comprised of the posterior fusiform gyrus (pFs, purple) as well as the lateral occipital area (LO, orange). The LOC extends medially until the border of the collateral sulcus (CoS). Areas are shown on an inflated cortex for the left (LH) and right ventral hemispheres (RH) as well as from a posterior-lateral view. Adapted with permission from "The topography of high-order human object areas", by R. Malach, I. Levy & U. Hasson, Trends in Cognitive Sciences, *6*(4), 176-184. Copyright 2002 by Elsevier Science.

Bottom-up models. Based on research with primates, IC processing may begin in striate and extra-striate cells, and proceed to higher-tier areas in a largely bottom-up manner. For example, using optical imaging, Ramsden, Hung, and Roe (2001) discovered that V1 patches activated by horizontal real contours were activated by vertical illusory contours, and V1 patches activated by vertical real contours were activated by horizontal illusory contours. Thus, the orientation of the IC (vertical or horizontal) activates opposing direction-specific areas in V1 that normally respond to real contours. To my knowledge, this is the only optical imaging study on IC processing and the only documentation of these activation-reversal effects. However, these findings are in line with several other studies suggesting that IC processing originates in the primary visual cortex rather than in higher-tier cortical areas (Eriksson & Nyberg, 2009; Maertens, Pollmann, Hanke, Mildner, & Möller, 2008; Montaser-Kouhsari, Landy, Heeger, & Larsson, 2007; Seghier et al., 2000; Sheth, Sharma, Rao, & Sur, 1996).

Perhaps more consistently than V1, V2 region has been implicated as the first area influenced by ICs, or at least influenced to a greater extent than V1 (Seghier & Vuilleumier, 2006). For example, Ffytche and Zeki (1996) used PET to examine regional cerebral blood flow (rCBF) in response to Kanizsa triangles and control stimuli (pacmen mouths rotated outwards). Results showed that rCBF was greatest for ICs compared to both control stimuli and that these differences occurred in V2 not V1. Interestingly, no IC effect was observed outside of the occipital lobe. Based on these results, the authors suggest that IC processing takes place in V2, and that boundary completion processes do not require recruitment of regions outside of the occipital cortex.

Arguably the most influential animal study on ICs was conducted by Heydt, Peterhans, and Baumgartner (1984). In their study, orientation-sensitive cells in the primate V2 area responded to ICs in the same ways as real contours, even though no luminance change actually fell on the cells' receptive field. Furthermore, changes to the stimuli that affected the strength of the illusion similarly affected neuronal responses. Results indicate that the critical components of the IC effect are the corners and line ends placed on either side of a cell's receptive field. The authors state that corner and line ends are coded first in V1 and converge on cells in the V2 area which have the ability to extrapolate boundaries that may belong to the same object. In later work, the authors downplay the role of higher-tier cortical areas stating that the reproducibility of the cell's responses (being stimulated over and over again with no change in response magnitude) as well the short latencies argue against cognitive effects (Heydt & Peterhans, 1989). Taken together this implies a bottom-up account of the IC phenomenon. This is consistent with other studies finding stronger IC effects in the V2 area relative to other brain regions (Hirsch & DeLaPaz, 1995; Peterhans & Heydt, 1989).

Top-down models. On the other hand, many recent human neuroimaging studies (fMRI, MEG, and EEG), find downstream object recognition areas, such as the lateral occipital complex (LOC), to be the neural locus of IC formation (Murray, Imber, Javitt, & Foxe, 2006; Murray et al., 2002; Pegna, Khateb, Murray, Landis, & Michel, 2002; Shpaner, Murray, & Foxe, 2011; Stanley & Rubin, 2003; Yoshino et al., 2006). While not denying effects in lower-level cortices, these authors conclude that striate and extrastriate activity relating to ICs is most likely a result of feedback from the LOC (Seghier & Vuilleumier, 2006).

EEG and MEG possess high temporal resolution compared to hemodynamic techniques and are therefore able to distinguish the stages of IC processing as well as address feedforward/feedback models. Using MEG with its source localization techniques, Halgren, Mendola, Chong, and Dale (2003) found that IC effects evoke strong activity 155 ms post stimulus and are localized to the LOC. There were effects at 110 ms in the extrastriate regions; however, the authors point out that these effects were relatively small and likely arose from low-level retinotopic differences between the Kanizsa and control stimuli. Furthermore, they found later effects at 230 ms in V1/V2 and suggested that this may reflect feedback from the LOC. A series of EEG studies combined with source localization techniques also localize the IC effect to the LOC, with peak effects around N170 ERP component (Murray, Foxe, Javitt, & Foxe, 2004; Murray et al., 2006; Pegna et al., 2002). This is in line with other papers showing larger N170 amplitudes to Kanizsa versus control figures (Herrmann & Bosch, 2001; Murray & Herrmann, 2013). Although ICs appear to affect the N170, other ERP components such as the P1 (Ikeda, Kirino, Inoue, & Arai, 2011), as well as the P3 (Böttger, Herrmann, & von Cramon, 2002), have been implicated. Taken together, these studies suggest that the LOC is responsible for boundary completion and object segmentation and that this process likely represents itself at the scalp as an N170 effect (Murray et al., 2006; Murray et al., 2002; Pegna et al., 2002; Shpaner et al., 2011; Stanley & Rubin, 2003; Yoshino et al., 2006).

The evidence herein suggests an interplay between lower- and higher-tier visual processing regions. In fact, many authors have commented on the role of feedforward/feedback processes between the V1, V2, and the LOC (Knebel & Murray, 2012; Maertens et al., 2008; Michel et al., 2004; Montaser-Kouhsari et al., 2007; Murray et al., 2002; Pegna et al., 2002;

Ramsden et al., 2001; Shpaner et al., 2011; Stanley & Rubin, 2003; Yoshino et al., 2006) and in a recent review, Murray and Herrmann (2013) expressed the need for future studies to examine the role of top-down and bottom-up factors during IC processing. Testing the putative role of top-down and bottom-up processing is difficult to do for the practical reasons of not being able to cleanly isolate each factor. However, a technique known as dichoptic fusion (described below) has been shown to effectively isolate bottom-up processing, allowing for more informative statements to be made about the nature of experimental effects with respect to top-down and bottom-up influences.

Developed by Moutoussis and Zeki, (2002), dichoptic fusion allows otherwise visible stimuli to become invisible to the participant. A basic description of the method is as follows: To one eye, a green stimulus on a red background is presented. At the same time, an identical stimulus (but with the foreground and background colours reversed), is presented to the other eye. With the help of prism lenses, the two monocular stimuli are refracted inward and seen as one stimulus in the middle of the screen (i.e., they are binocularly viewed). Importantly, the red and green colours in each monocular stimulus partially cancel each other out at the binocular level, leading to the perception of a solid yellowish patch. The true content of the stimulus impinges on the retina and in fact activates many cortical areas (Moutoussis & Zeki, 2002; Schurger, Pereira, Treisman, & Cohen, 2010), despite not being consciously perceived. When colour fusion is successful, top-down awareness relating to the stimulus is blocked. However, to allow top-down awareness of the stimulus, identical images may be presented to each eye (with no reversal of foreground and background colours). When viewed binocularly, the stimuli will not cancel each other out, and the stimulus content is readily perceived. For example, using this

method in a face/house comparison, a previous fMRI study showed greater fusiform activity for faces compared to houses, even when the participant was unaware of the stimulus differences due to the dichoptic colour fusion (Moutoussis & Zeki, 2002). Dichoptic fusion is therefore a promising method for addressing questions of bottom-up versus top-down contributions to a particular brain function.

The Current Study

The current study will record high-density EEG to Kanizsa figures and control stimuli. Dichoptic fusion will be used to isolate electrocortical activity relating to the bottom-up processing of ICs. To the best of my knowledge, dichoptic fusion has not yet been used in EEG research. However, extrapolating from the fMRI studies above, my study will examine three hypotheses:

(1) Kanizsa figures will elicit larger N170 than control (misaligned Kanizsa) stimuli in general (i.e., when no dichoptic fusion is used). This is a validity check of these stimuli.

(2) Larger N170 amplitudes will occur even when stimulus features are not known by the participant (by means of dichoptic fusion). If this second hypothesis is supported, evidence of purely bottom-up IC processing would be demonstrated, supporting the role of bottom-up processing independent of top-down contribution.

(3) The top-down model predicts an interaction such that the awareness factor will interact with the Kanizsa illusion and influence the N170. If this is the case, we must reject a strong bottom-up model of illusory contour processing.

Methods

Dichoptic Fusion

The explanation of dichoptic fusion given above is rather simplistic. In reality, achieving reliable colour fusion is not easily accomplished. Many crucial details in the process have not been well-documented. In the following sections I will describe the further crucial steps that were taken to obtain reliable colour fusion in this experiment: Heterochromatic Flicker Photometry (HFP), dithering, and the use of prism lenses. As in Moutoussis and Zeki (2002), the current study used stimuli having red and green as the two colours that were to fuse into yellow when viewed binocularly.

Heterochromatic flicker photometry

One issue that is necessary for reliable colour fusion is that the reds and greens must be subjectively isoluminant (i.e., perceived as being equally bright). When two colours, in this case red and green, are identical in every way except for hue (i.e., they contain identical intensity and shading levels), they are said to be objectively isoluminant. Subjectively though, one will always perceive green as brighter then red, and therefore the colours cannot be considered subjectively isoluminant [3]. This subjective difference will lead to unsuccessful colour fusion, so the luminance of the green must be adjusted downward until it is perceived to be as bright as the red. This was accomplished by using Heterochromatic Flicker Photometry (HFC) (Siegfried, Tepas, Sperling, & Hiss, 1965). Specifically, the red and green colours used in the experiment were set to alternate, one after the other, rapidly on a computer screen (~30Hz). A button was then pressed which lowered the luminance of the green patch by a small amount. When the two patches

[3] Green may be perceived as brighter than red because both M and L type cones in the retina maximally absorb wavelengths between 530-560*nm*, which correspond to colours ranging from green to yellow. Red colour absorption from these cones is markedly less (Purves et al., 2001).

become subjectively isoluminant, the flicker between red and green is minimized (i.e., the two patches appear to smoothly transition from one to the other at a much slower rate) (Schurger et al., 2010; Siegfried et al., 1965). A second button is pressed to indicate when subjective isoluminance has occurred, and the red and green values are then stored. This was repeated for 50 different red and green contrast levels (described below). Ideally HFC would be done for each individual participant as not all visual systems would achieve subjective isoluminance at the same level of green. However, this would have increased the time to complete the experiment substantially. Instead the stimuli were made isoluminant to the experimenter only. Informal testing with some of the participants indicated that the flicker was minimized at very comparable levels across individuals and so HFC was deemed unnecessary. This same inter-subject consistency of the subjective isoluminance point was also noted in another dichoptic fusion study (Schurger et al., 2010).

Dithering

In order for the pacmen shapes in the foreground to blend together and cancel out at the binocular level, they must be slightly blurred. Otherwise, sharp edges in the stimulus will lead to edge artifacts in the binocular image and colour fusion will not be achieved. However, conventional Gaussian blurring introduces intermediate shades. In this case a greenish red colour would have to be added to the stimuli to create a blurred effect on the pacmen shapes. These additional shades will be in common between the right and left monocular stimuli, thus when viewed binocularly the edges of the pacmen shapes in each eye would not fully cancel each other out. This is because total colour fusion requires that each eye sees the exact inverse colouring of that of the other eye. In fact this works best if the stimuli are only made up of only two colours

(e.g., red and green with no intermediate colours) (Schurger, 2010). To circumvent the problem of introducing intermediate colours that would be in common between each eye, blurring is done by dithering the image. Dithering refers to the reduction of pixel densities near edges to create a blurred effect. Therefore dithering blurs the image without adding additional shades beyond the isoluminant red-green pair (see Figure 2).

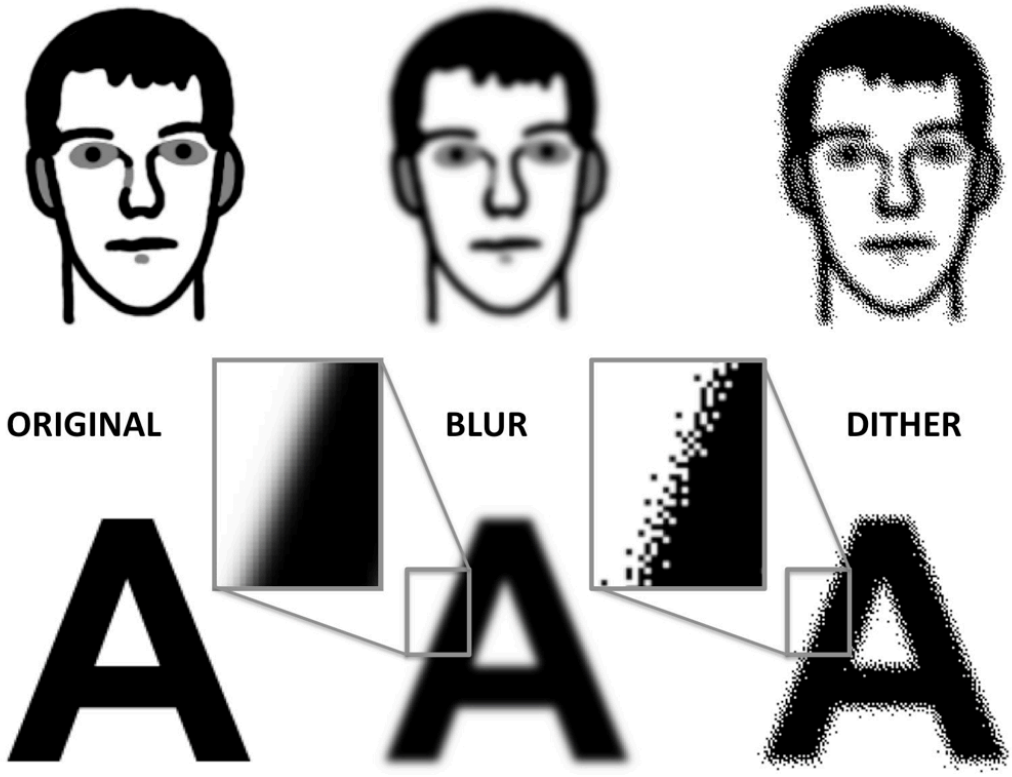

Figure 2. Example of Gaussian blurring versus dithering. Gaussian blurring (middle image) introduces intermediate shades, whereas dithering only manipulates the pixel densities to create a blurred effect (Copyright 2015 Aaron Schurger. Reproduced with permission).

Prism lenses

In order to view the right and left stimuli as one binocular image, prism lenses were used. The prism lenses in this experiments refracted light from the periphery towards the fovea, allowing the right and left stimuli to converge onto one another and be perceived as a single image in the center of the screen[4]. The prism lenses must be constructed to suit the size and binocular disparities of the left and right stimuli. In this experiment, lenses were cut so that what was seen by the left and right eye appeared shifted ~3.5˚ towards the center of the screen (see Figure 3).

[4] Normally lenses require a prescription, however, after explaining what the glasses were going to be used for, a local lens maker agreed to make them without a prescription.

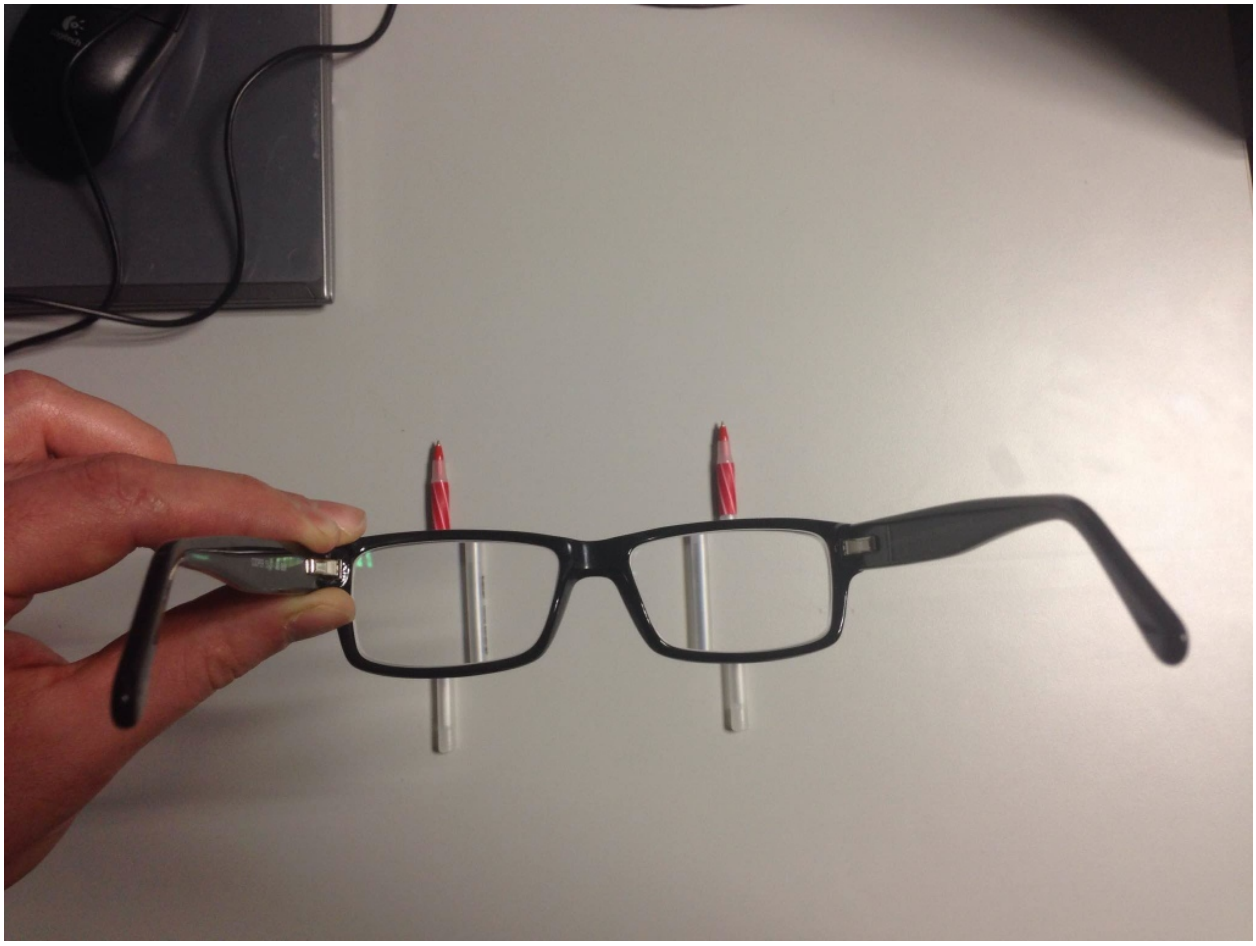

Figure 3. The properties of the prism lenses used in this experiment. Light from the left lens is refracted 3.5 DVA to the right and light from the right stimuli is refracted 3.5 DVA to the left. When Kanizsa and control stimuli are viewed with such glasses, they are seen as one central image by the participant.

For this experiment lenses were cut with 6.1163 diopters of prism (~3.5 DVA) correction[5]. The lenses were also base-out (meaning that the thick part of the lens points towards the temple allowing the light to be refracted inward towards the fovea rather than outward towards the periphery) and had anti-glare coating. Prism lenses with diopter corrections such as these are relatively robust to a range of binocular disparities as well as differences in head size and other features of the face (Erkelens & Regan, 1986).

Participants

Twenty-three healthy graduate and undergraduates students from Brock University participated in this study (9 females, mean age = 26, range 18-31 years). All participants reported normal or corrected-to-normal vision (by contact lenses). Participants were screened for head injuries. An honorarium was given to the participants for their time. Four subjects reported difficulty maintaining one central stimulus (the fusion between the right and left images) for long periods of time. Since this is a prerequisite for the desired colour fusion, and there was no way to know which trials were affected, these subjects were not analyzed. Upon inspection of the ERP envelopes, three subjects failed to show the classic P1-N170-P2 complex or associated topographies. Two of these subjects had lost approximately 75% of the total number of trials during the artifact reject procedure described below. These subjects were removed bringing the total N to 16. No statistical analyses or visual comparisons of condition waveforms at particular sites were done prior to removing outliers, to ensure the results would not be biased.

---

[5] Lens makers use the term ‘prism diopters’ for what vision scientists refer to as degrees of visual angle (DVA) and there is a formula to convert between the two (roughly speaking, 1 DVA = 1.75 prism diopters) (Shurger, 2009).

Stimuli

Kanizsa squares and triangles were used to elicit ICs. The control figures were identical but had the pacmen mouths turned outward to disrupt ICs. Pacmen shapes were either red and set on a green background, or green and set on a red background. The exact intensities of the reds and greens relative to one another (i.e., contrast) varied along a continuum (high to low contrast) and is described in detail below). To add variability to the set, versions that were rotated 45° were also used (producing a diamond IC). A thin blue border and small fixation point were also added. The right and left stimuli subtended roughly 6° and were separated by ~1° which gave room for a divider that separated the right and left visual presentations. Stimuli were created using GNU image manipulation program (GIMP), as well as MATLAB (Mathworks, MA).

Design and procedure

Aligned conditions elicited the ICs, and the misaligned conditions were the controls. When the same red and green pair was presented to each eye, allowing perception of the stimulus content, the condition was referred to as ‘same’. The ‘opposite’ condition occurred when opposing red and green pairs were presented to each eye, preventing the perception of the stimulus. All red and green combinations were counterbalanced across eyes. Thus, there were four conditions in a 2x2 within-subjects design: (1) aligned same (AS), (2) aligned opposite (AO), (3) misaligned same (MS), and (4) misaligned opposite (MO) (see Figure 4).

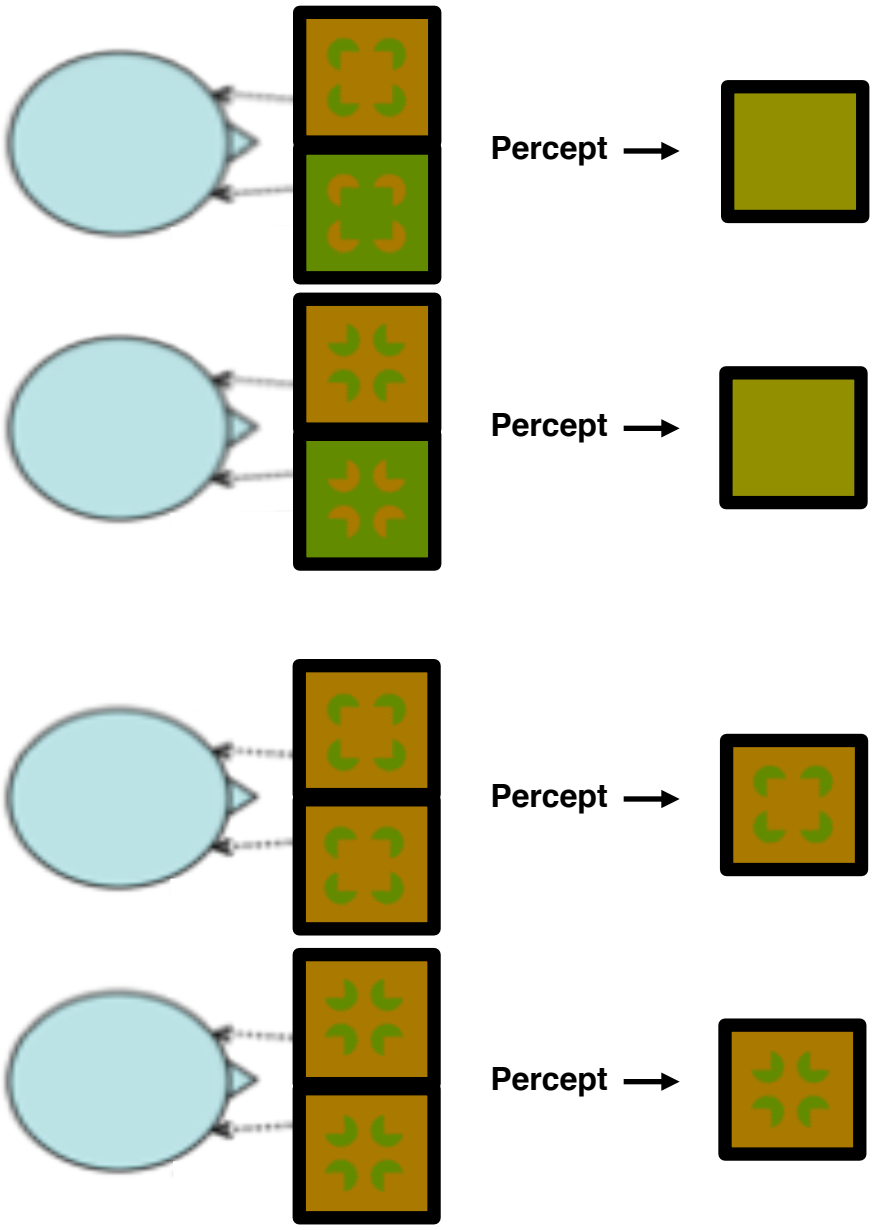

Figure 4. Top panel shows Kanizsa (aligned) and control (misaligned) in the opposite conditions. Bottom panel shows the same but for the same conditions. The schematics on the show the configuration of the prism lenses, refracting light from each monocular stimulus, which are separated by a divider.

Note that two other types of control conditions were used that did not include any pacmen shapes, but were simply blank red or green patches. Having no pacmen figures on them, these coloured patches allowed one to look at EEG in response to both eyes being stimulated with the same colour versus stimulation from the opposite colours in each eye. This is important because the low-level stimulation difference covaries with the manipulation of awareness, which is of primary interest in dichoptic fusion paradigms. Moutoussis and Zeki (2002) subtracted the BOLD response from these conditions from that of the face and house conditions to isolate activation that was face/house specific. However, due to the pattern of results that will be described later, the analysis of these types of control stimuli was unnecessary. There were 200 trials in each of the four experimental condition and 150 trials for each of the blank control conditions (same and opposite), giving 1100 trials in total. The experiment lasted about 40 min, divided into 10 short blocks with breaks in between.

Participants sat in a dimly lit, sound-attenuated room. Stimuli were presented using Psychtoolbox on a Dell CRT monitor with 1024 X 768 screen resolution and 60 Hz refresh. Stimuli were presented pseudo-randomly on the computer screen. Each trial was presented for 150 ms with a random ISI of 800-1000 ms. The task for the participants was to indicate on each trial whether or not they saw pacmen. They were instructed to respond as quickly and accurately as possible via a button press. The button presses were counterbalanced across participants. Once the decision was made, the next trial would commence. Prior to EEG recording, a practice block of twenty-five trials was completed by the participant in order to familiarize them with the dichoptic fusion set up.

Dichoptic fusion experiments typically include dozens of different red and green pairs, each with a different level of contrast (Schurger, 2010; Moutoussis & Zeki, 2002). This is due to the fact that, in general, high colour contrasts do not fuse (binocular rivalry happens instead), but as indicated earlier not all individuals will fuse at the exact same contrast level. Unfortunately, adding dozens of levels of contrast is impractical as it increases the number of trials and length of the experiment exponentially. In the current experiment contrasts levels between reds and greens were adjusted using a 1-up-1-down adaptive staircase procedure with fixed step sizes (Ehrenstein & Ehrenstein, 1999). Contrast adjustments were made based on the following two contingencies: (1) If participants indicated that they had seen pacmen in the opposite condition, meaning that colour fusion was unsuccessful, the colours were adjusted to have lower contrast in the subsequent trials and (2) if participants indicated that they had not seen pacmen in the same condition, meaning that contrast was below perceptual threshold, the colours were adjusted to have higher contrast in the subsequent trials (see Figure 5). The levels of contrasts were constructed prior to the experiment as follows: Beginning at a red, green, blue (RGB) value of R=.5, G=.5, B=0, a red colour was created by increasing the R value by .002 and decreasing the G value by the same amount. The R and G values were then switched to create a green colour. This was repeated fifty times leading to fifty symmetrical red and green colours with a maximum red value of R=.6, G=.4, B=0 and a minimum red value of R=5.020, G=.4980, B=0. The G values at each of the fifty levels of green were then adjusted down via HFP as described above. At the outset of the practice block an arbitrary red/green contrast level was chosen (the 25th level) as a starting point. The adaptive staircase procedure continued cumulatively throughout the entire experiment, including the initial practice block. Only trials with a desired outcome were

analyzed (i.e., opposite trials when pacmen were not reported and same trials when pacmen were reported).

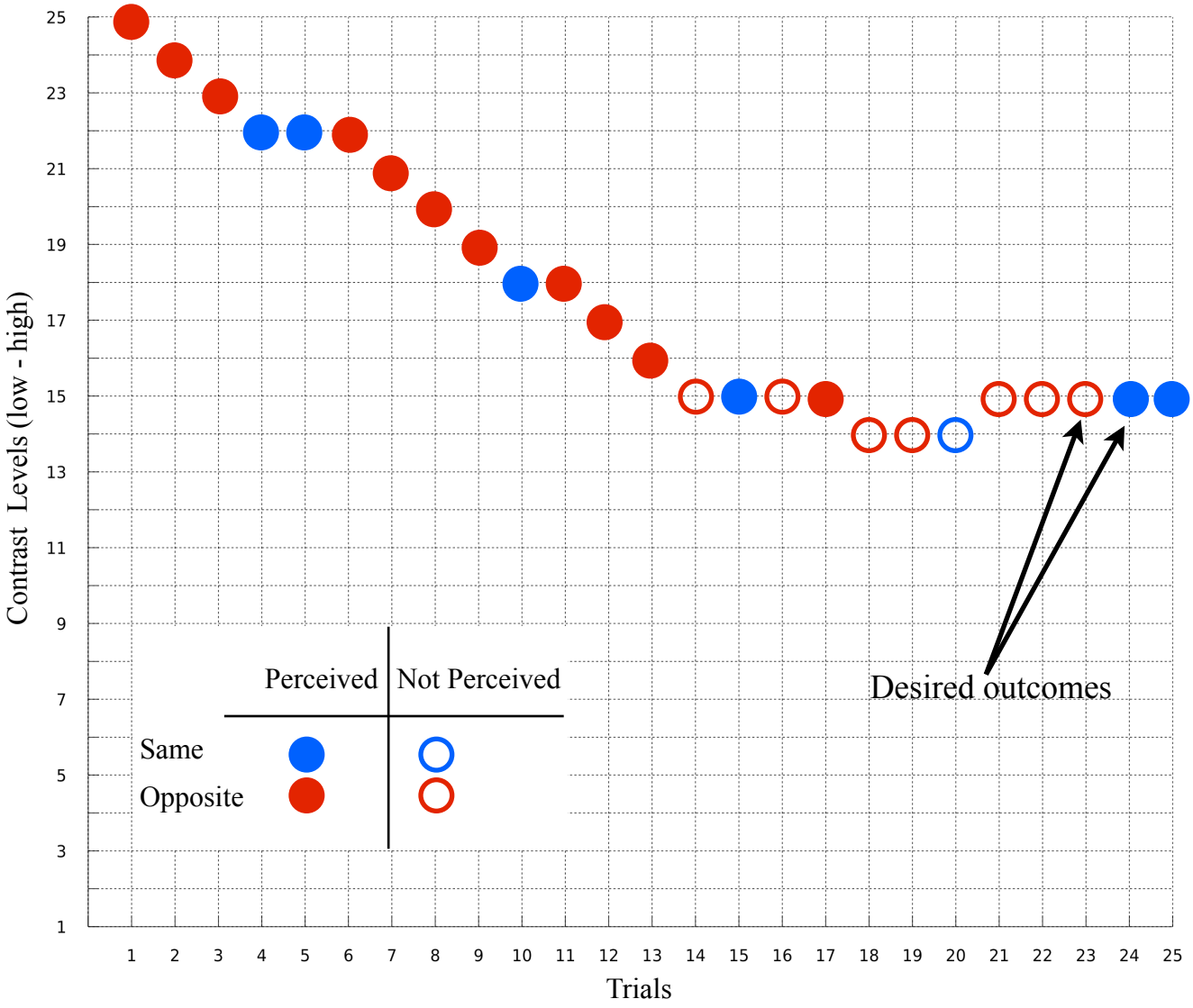

Figure 5. Example of the 1-up-1-down adaptive staircase procedure used in the current experiment. Contrasts levels between red and green were adjusted based on the following contingencies: (1) If participants reported seeing pacmen on opposite trials, contrast was reduced and (2) if they reported not seeing pacmen on same trials, contrast was increased. If the desired outcome was met (i.e., not seeing pacmen in opposite trials, and seeing them in same trials), the contrast remained unchanged in subsequent trials. Only the trials with desired outcomes were analyzed.

EEG recording

EEG data were recorded from a BioSemi ActiveTwo system with 135 scalp channels, 7 of which were placed around the eyes to record ocular activity (see Figure 6). The signal was low-pass filtered online at 512 Hz. Electrode offsets (i.e., a measure of the signal quality which can be interpreted similarly to impedance measurements) were maintained below 50 μV.

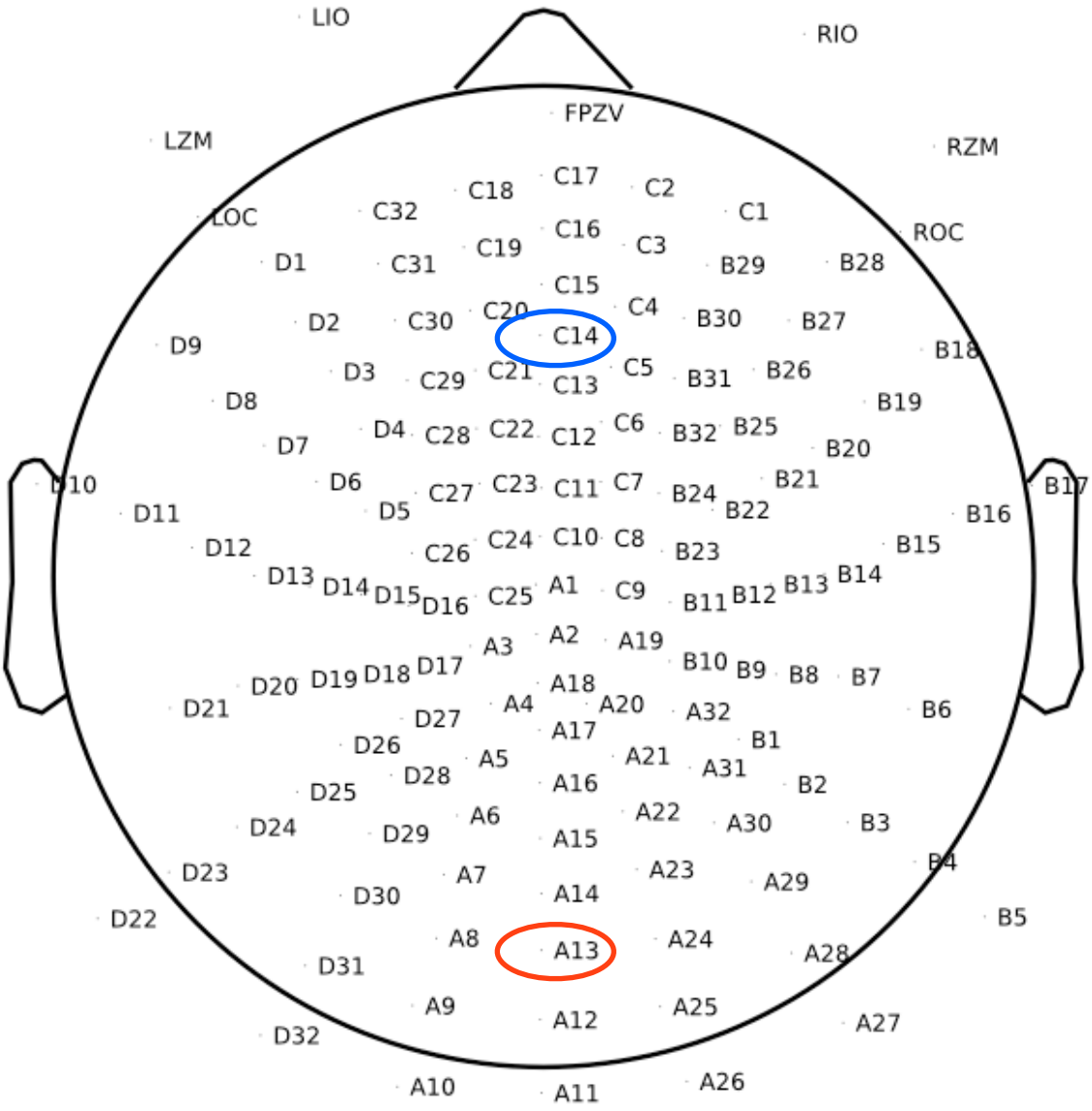

Figure 6. Montage diagram of 128 evenly spaced scalp sensors and 7 sensors for recording ocular activity. The actual locations of sensors are to the left of the labels. In later sections, ERP waveforms are shown at sites corresponding approximately to Oz and Fz (red and blue circle respectively) and topographic statistics are displayed for all sites at latencies of the maximum effect.

EEG preprocessing

EEG preprocessing was accomplished inside of MATLAB using both native EEGLAB (Delorme & Makeig, 2004) functions as well as an automated artifact removal procedure developed by Desjardins and Segalowitz (2013). All of the computationally intensive processing steps ran on the Shared Hierarchical Academic Research Computing Network (SHARCNet). For each subject, breaks and clearly bad channels were manually removed and a .1-30 Hz filter and average rereference were applied. Further bad channels (including linked channels) and noisy time periods were removed using the automated artifact removal procedure (Desjardins & Segalowitz, 2013). Independent Components Analysis (ICA) (extended Infomax) (Bell & Sejnowski, 1995) was then run on each subject. Independent components with topographies and time courses corresponding to eye blinks, heart activity, muscle activity, or line noise, were manually rejected. All other components that could not be readily identified as a one-of-a-kind biological artifact or pure line noise, were left in the data as we could not justify their removal in case they were mixtures containing real cortical data. The remaining ICA activations were then multiplied back to the scalp resulting in scalp data that were cleansed of biological artifacts. Finally, the data were segmented to the onset of the stimulus in each condition. The baseline removal period was -200 ms to 0 ms relative to stimulus onset.

One intuitive way to assess whether the ICA decomposition is stable and usable for hypothesis testing is to run the ICA multiple times on the same data to see whether the same components are consistently outputted (Delorme & Makeig, 2004). Following the initial ICA run, I reran ICA twice more, and for the majority of subjects, only blink and heart components were consistently replicated. Therefore, following the recommendation in Delorme and Makeig

(2004), the remaining unstable components were deemed uninterpretable and hypothesis testing using sources was abandoned in favor of a traditional scalp-level analysis.[6]

Statistical analyses at the group and single-subject level

Percentile bootstrap tests using 20% trimmed means (Wilcox, 2013) were conducted on every scalp channel and every time point, at the group and single-subject level (Desjardins & Segalowitz, 2013; Rousselet, 2008; Oruc, 2011).[7] This was accomplished inside the STATSLAB software suite (Campopiano, 2014). Compared to traditional t-tests, percentile bootstrap tests using trimmed means, lead to substantial increases in power and improved control over Type I error (Berkovits et al., 2000; Nevitt 2000; Keselman et al., 2004; Keselman et al., 2003; Wilcox et al., 2000; Wilcox & Keselman, 2003; Wilcox, 2010). Given the prior N170 effects found for Kanizsa figures, the results will focus primarily on occipital channels (nearby and including Oz).

Single-subject percentile bootstrap tests were conducted by resampling with replacement from the single-trials, leading to a new set of EEG trials. ERPs were calculated using the 20% trimmed mean at each time point and channel. The single trials were resampled 1000 times, yielding 1000 ERP waveforms for each channel. Difference scores were taken for all pairwise comparisons and the interaction by multiplying the data by the appropriate contrast coefficients (Wilcox, 2013). Conditions were labeled as (1) aligned same, (2) aligned opposite, (3) misaligned same, and (4) misaligned opposite. To compare conditions one and three, the contrast coefficients would be [1 0 -1 0]. To test for an interaction we used [1 -1 -1 1], which is

---

[6] ICA decompositions can fail for several reasons: (1) poor stationarity in the data possibly due to low frequency drifts, (2) muscle and/or line artifacts that end up being mixed into output components when they lead to more spatial sources than there are channels, and (3) nonlinearities (i.e., the data are not a linear sum of the source projections) that occur when large amplitudes lead to signal clipping (Delorme & Makeig, 2004).

[7] A mass univariate approach is frequently done in fMRI research, but not in EEG, which tends to focus only on small time windows and a small number of channels. Mass univariate approaches are however recommended for EEG data (Grope, 2011), especially as software and computing power improve.

equivalent to the difference of the differences. Bootstrapped difference scores were then sorted in ascending order as follows where $B = 1000$, $D^*_{(1)} \leq \ldots \leq D^*_{(B)}$. A $1 - \alpha$ percentile bootstrap confidence interval was then calculated by letting the lower bound $l = \alpha B/2$ rounded to the nearest integer, and setting the upper bound $u = B - l$ yielding

$$(D^*_{(l+1)}, D^*_{(u)}).$$

For example, since there were 1000 resamples in this experiment, the upper bound of the 95% CI would take the 975th value in the sorted bootstrap values. The lower bound would take the 26th value in the sorted bootstrap values [8]. This approach was extended to the group level analysis by simply averaging all subjects' bootstrapped ERPs together, which led to B grand averages for each condition. $1 - \alpha$ confidence intervals can be taken around the grand average differences in the same way as in the single-subject case (Wilcox, 2013; Desjardins & Segalowitz, 2013; Rousselet, 2008; Oruc, 2011). Alpha was set to 0.05 for all statistical tests (see Figure 7).

[8] Single-subject bootstrap tests are more powerful than group-level tests because the subject themselves provide the only source of variance for the statistical comparison (not including measurement error). Furthermore, this approach is the only way to show how statistically consistent the subjects are to the group results, providing a complementary view of the data. These were the primary reasons for including single-subject statistics, just as others have done in previous studies (Rousselet et al., 2008; Desjardins & Segalowitz, 2013).

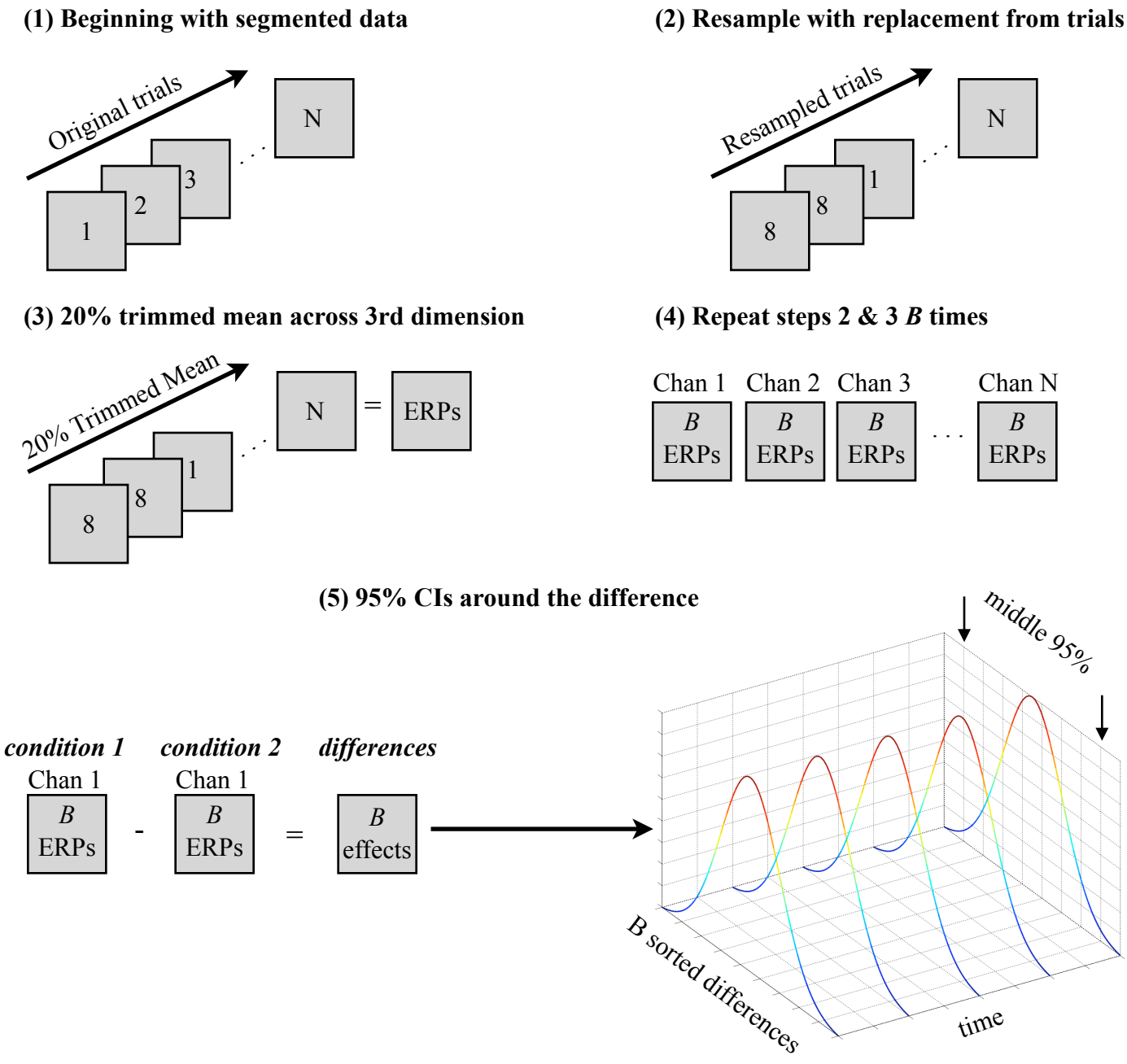

Figure 7. Graphical representation of the percentile bootstrap procedure based on resampling with replacement from single trials. The middle 95% of the sorted bootstrap differences define the upper and lower bounds of the 95% CI (Wilcox, 2013; Rousselet, 2008). Note that the tails of the bell-shaped distributions are lined up with each other only for visual simplicity.

Results

Results are organized by group comparisons at the time of the N170, followed by the identical comparisons at the single subject-level. Tests for Hypotheses One (AS-MS) and Two (AO-MS) are described first, followed by three addition tests not associated with a particular *a priori* hypothesis (AS-AO, MS-MO, and the interaction). Finally, later effects in the P3 latency range are laid out in the same manner.

N170 effects

Group-level results for AS-MS. To test Hypothesis One, I examined the effect of ICs when participants reported seeing pacmen. I found a statistical increase in N170 amplitude for aligned compared to misaligned same conditions. This effect extended temporally from about 140-180 ms and spatially across central occipital channels (see Figure 8). The maximum mean difference had a latency of 152 ms and was located at Oz. The confidence interval (CI) around the mean difference at Oz indicates a small effect size (M = .8; 95% CI = [-1.4 -0.4], p<.05). Note that no P1 or P3 differences were found comparing aligned same to misaligned same conditions as others sometimes find in other paradigms (Ikeda et al., 2011; Böttger et al., 2002).

Single-subject results for AS-MS. Single-subject comparisons of aligned same versus misaligned same conditions revealed highly variable effects across subjects, both spatially and temporally. Only five of 16 subjects show statistically larger amplitudes for aligned same relative to misaligned same conditions between 140-180 ms when measured at Oz. Eleven of 16 subjects are however pointed in the same direction as the group N170 effect, around the 150 ms mark. Note that Participant #9's CI and effect size are roughly five times larger than the rest of the

group. Removing this subject from the group analysis did not change the statistical outcomes, but did result in slightly smaller effect sizes (see Figure 9).

Group results for AO-MO. To look for bottom-up evidence of IC processing, testing Hypothesis Two, I examined the difference between conditions in which participants reported not seeing pacmen. There was no statistical difference for aligned compared to the misaligned opposite condition, whether at Oz ($M_{(152ms)}$ = .1; 95% CI = [-.5 .8], p>.05) or any other channel at 152 ms (see Figure 8).

Single-subject results for AO-MO. When looking at single-subject results for the aligned opposite versus misaligned opposite conditions, we again see highly variable results at Oz. Subject 16 shows a statistical effect between 140-180 ms but in fact this effect is in an unexpected direction (larger amplitude for misaligned opposite). Roughly six of 16 subjects have negative deflections between 140-180 ms (see Figure 10).

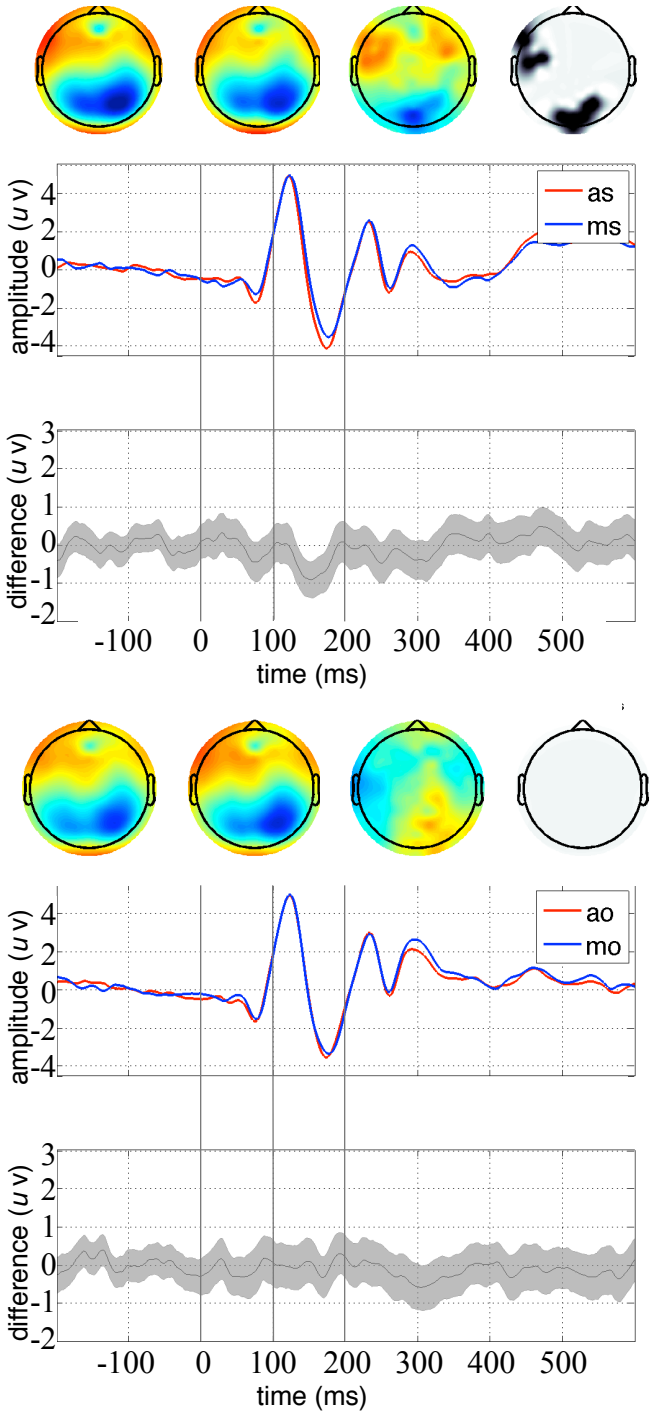

Figure 8. Top panel shows ERP waveforms measured at Oz comparing aligned same (as) and misaligned same (ms) conditions. The corresponding 95% CI around the difference is shown in gray. Topographic voltage differences and *p* values (<.05, black) are displayed at 152ms. The bottom panel shows the aligned opposite (ao) and misaligned opposite (mo) comparison.

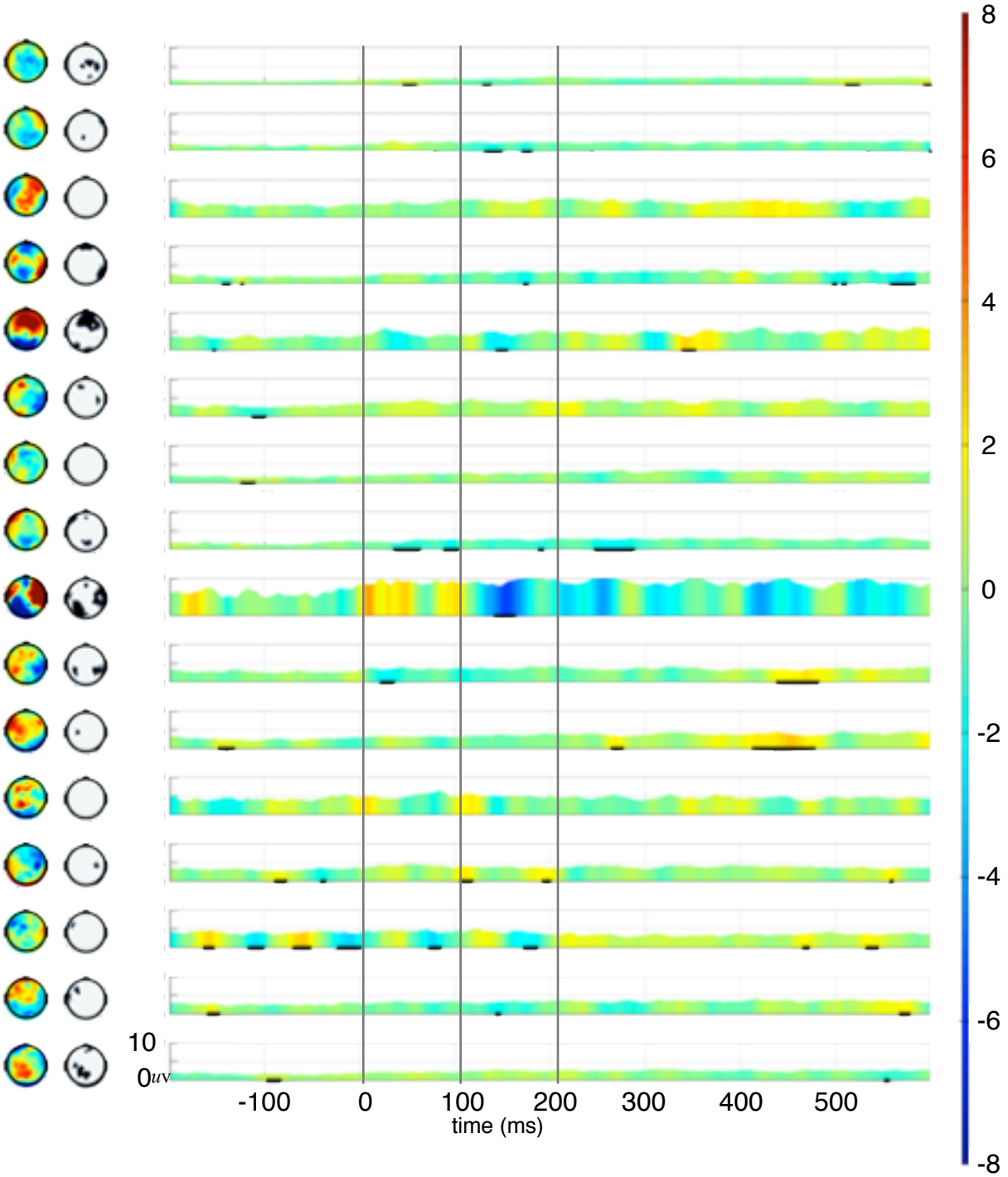

Figure 9. Single-subject results for aligned same versus misaligned same. Horizontal colour bars represent mean differences between conditions at Oz. The margin of error (MOE) is shown on the Y axis. Topographic voltage differences and *p* values (<.05, black) are displayed at 152ms.

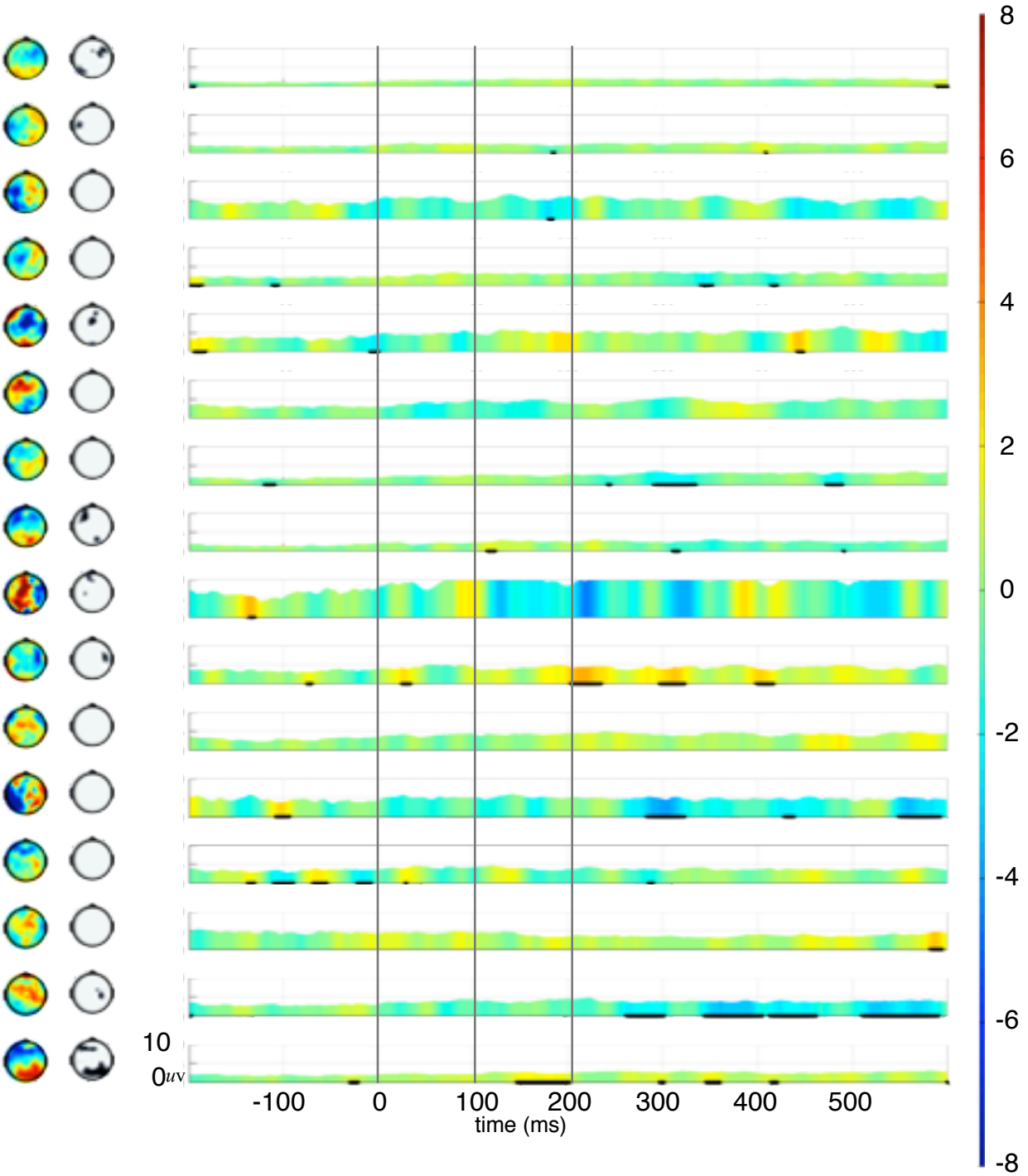

Figure 10. Single-subject results for aligned opposite versus misaligned opposite. Horizontal colour bars represent mean differences between conditions at Oz. The margin of error (MOE) is shown on the Y axis. Topographic voltage differences and *p* values (<.05, black) are displayed at 152ms.

Group-level results for AS-AO. When comparing aligned same versus aligned opposite conditions I found a statistical increase in N170 amplitudes (see Figure 11). This effect extended temporally from about 130-180 ms and spatially across occipital and parietal channels. The maximum difference had a latency of 149 ms when measured at Oz. The CI around the difference at Oz indicates a small effect size (M = .8; 95% CI = [-1.2 -0.25], p<.05).

Single-subject results for AS-AO. In the aligned same versus aligned opposite comparison, 12 of 16 subjects show negative deflections between 140-180 ms at Oz; however, only 3 of these subjects show a statistical difference. Subject 16 again shows a small statistical effect in the direction opposite from expectation around 120 ms (see Figure 12).

Group-level results for MS-MO. There was no statistical difference for misaligned same compared to misaligned opposite conditions for the N170 at Oz ($M_{(152ms)}$ = .2; 95% CI = [-.4 . 75], p>.05) (see Figure 11). Differences did arise spatially at 152 ms at various channels but they were not graded across contiguous sites and thus will not be interpreted. This can be justified because true ERP effects are expected to be spread across multiple adjacent sites when using a high density montage more than noise due to the nonzero spatial and temporal correlations of the underlying neural generators (Groppe et al., 2011).

Single-subject results for MS-MO. Six of 16 subjects show negative deflections in the 140-180 ms range for the misaligned same versus misaligned opposite conditions at Oz. Only 2 of these were statistical decreases. Subject 16 again shows a statistical increase ranging from 120-180 ms (see Figure 13).

Group-level interaction. Lastly, hypothesis three tested whether or not the awareness factor interacted with the Kanizsa illusion, as a top-down model would predict. Indeed this was

the case as the N170 amplitude was statistically larger for the AS condition relative to the other conditions (i.e., when awareness of the stimulus and the illusory formation co-occurred). This interaction extended temporally from about 145-155 ms and spatially across central occipital channels (see Figure 14). The maximum difference had a latency of 150 ms when measured at Oz. The CI around the difference at Oz indicates a small effect size (M = -1; 95% CI = [-1.8 -0.2], p<.05).

Single-subject interactions. For the interaction at Oz, roughly 10/16 subjects show a negative deflection from 140-180ms, which is consistent with the group interaction effect. However, in only roughly three subjects was this difference a statistical decrease (see Figure 15).

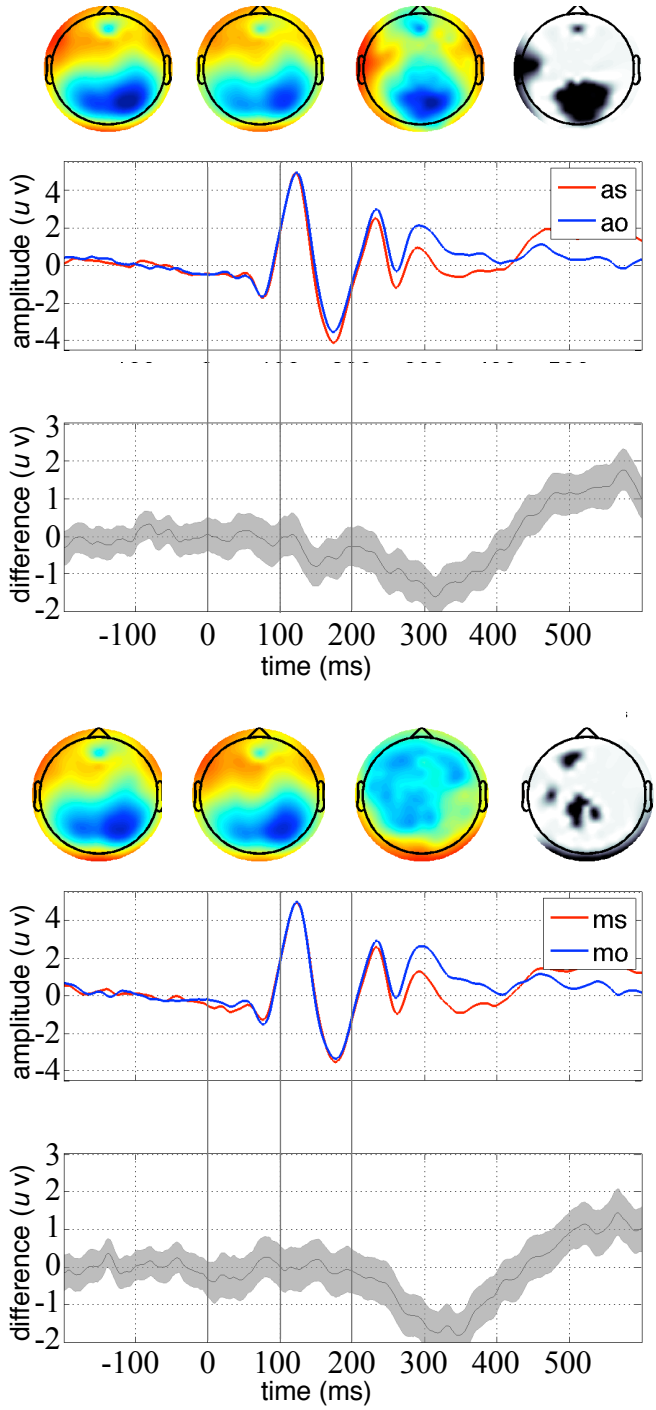

Figure 11. Top panel shows ERP waveforms measured at Oz comparing aligned same (as) and aligned opposite (ao) conditions. The corresponding 95% CI around the difference is shown in gray. Topographic voltage differences and *p* values (<.05, black) are displayed at 152ms. The bottom panel is identical but for the misaligned same (ms) and misaligned opposite (mo) comparison.

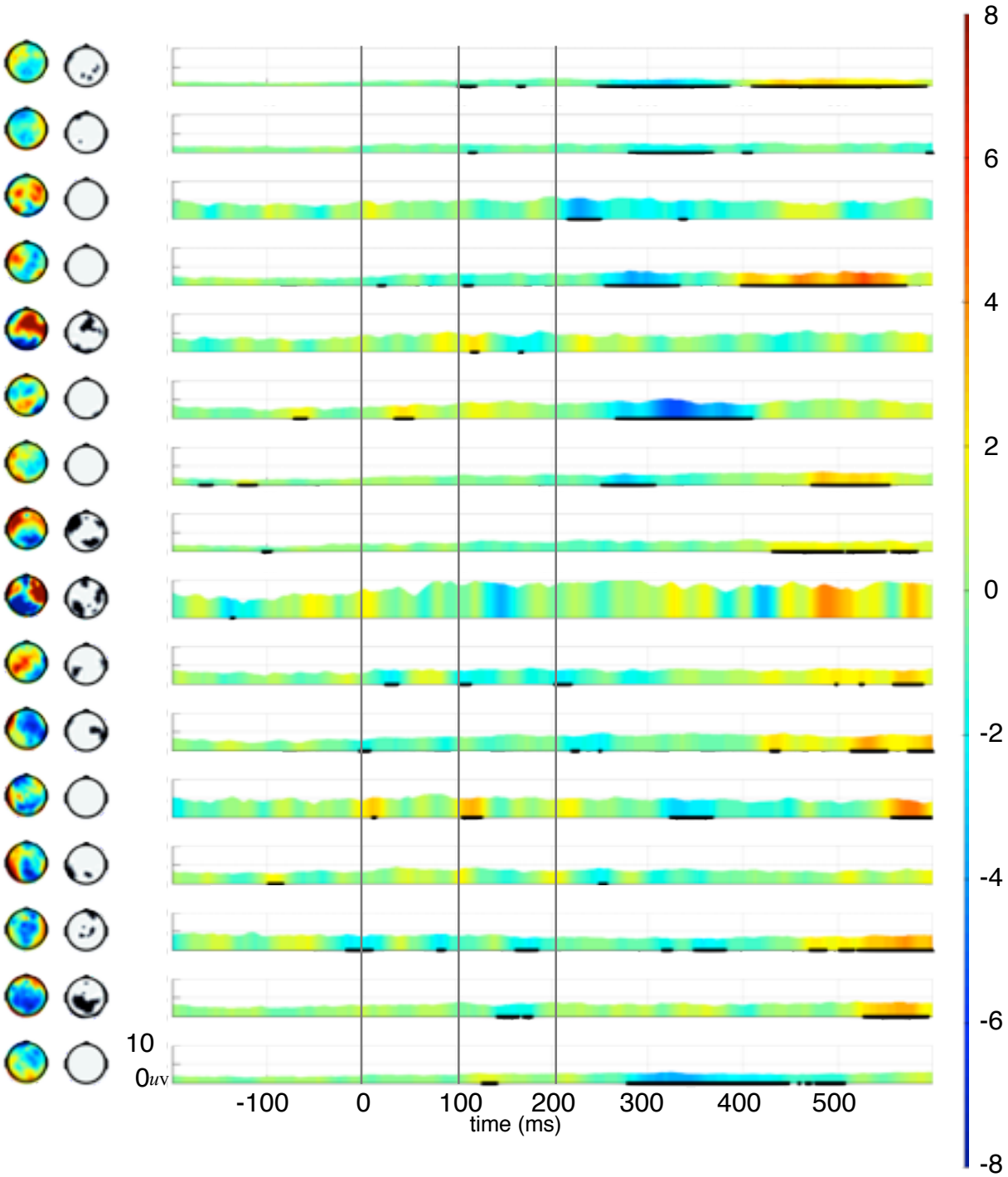

Figure 12. Single-subject results for aligned same versus aligned opposite. Horizontal colour bars represent mean differences between conditions at Oz. The margin of error (MOE) is shown on the Y axis. Topographic voltage differences and *p* values (<.05, black) are displayed at 152ms.

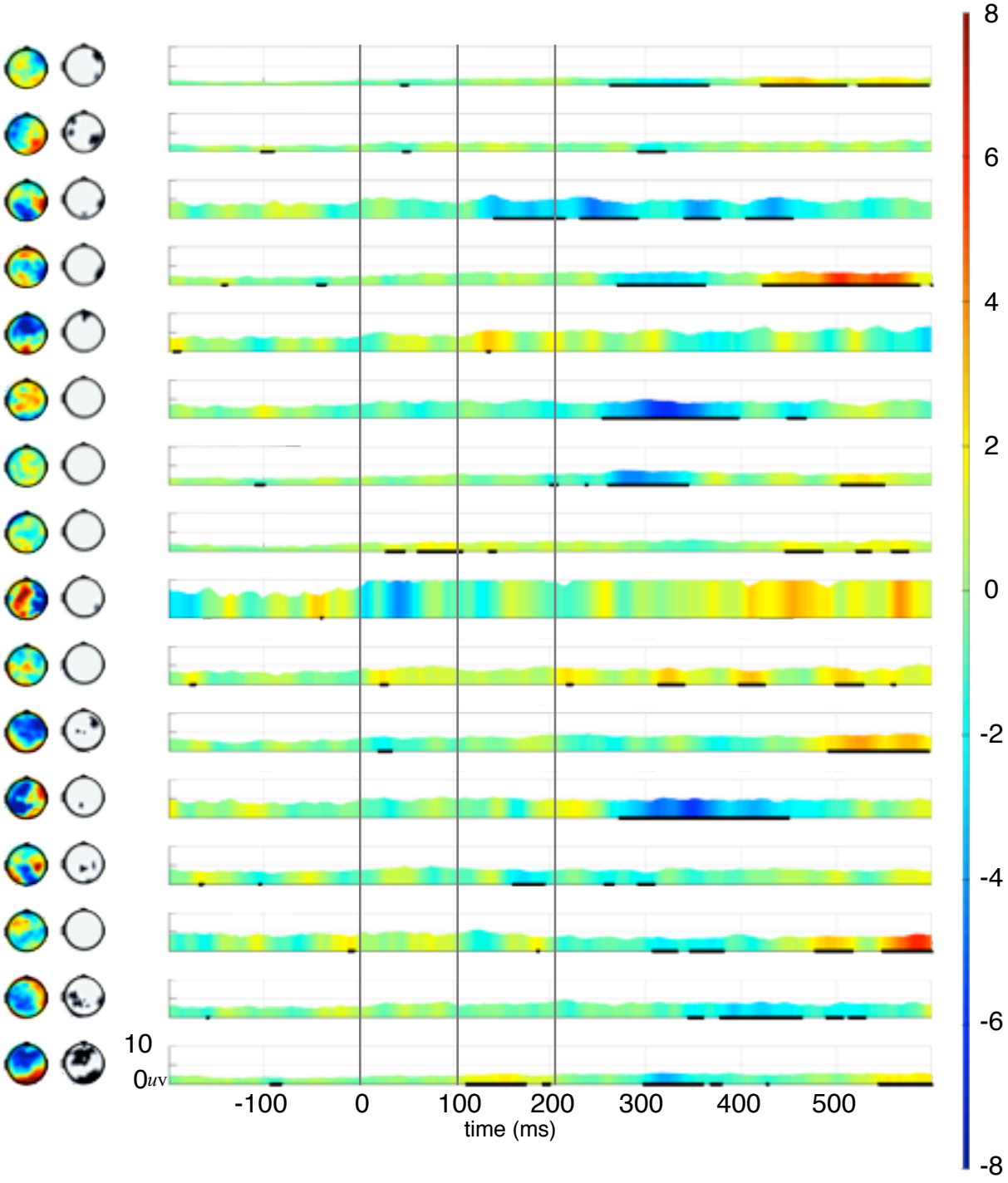

Figure 13. Single-subject results for misaligned same versus misaligned opposite. Horizontal colour bars represent mean differences between conditions at Oz. The margin of error (MOE) is shown on the Y axis. Topographic voltage differences and *p* values (<.05, black) are displayed at 152ms.

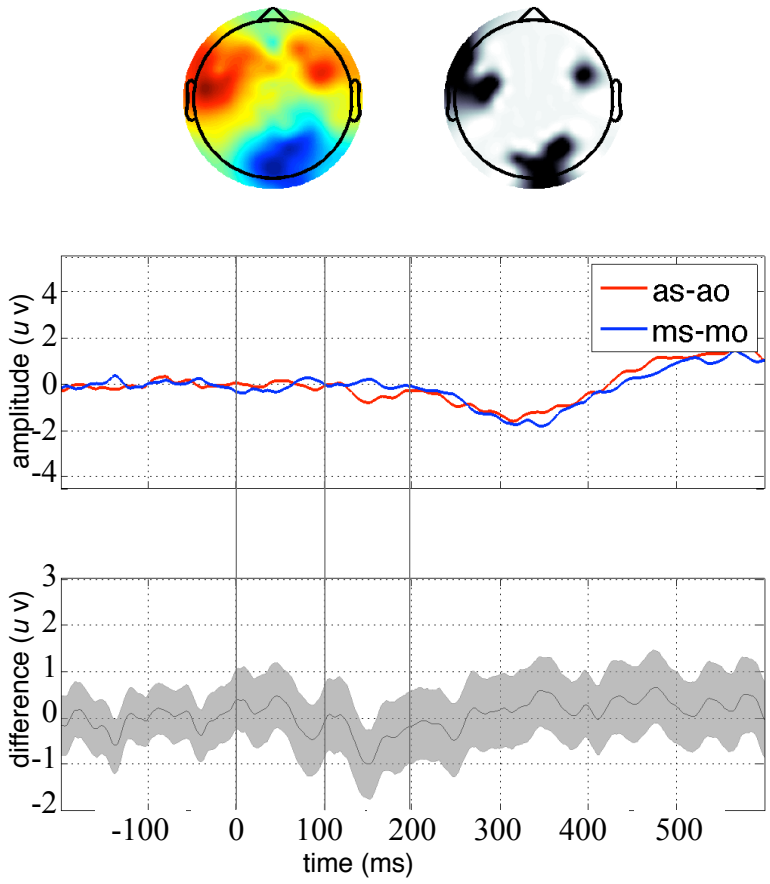

Figure 14. ERP waveforms measured at Oz for the interaction. The corresponding 95% CI around the difference is shown in gray. Topographic voltage differences and *p* values (<.05, black) are displayed at 152ms.

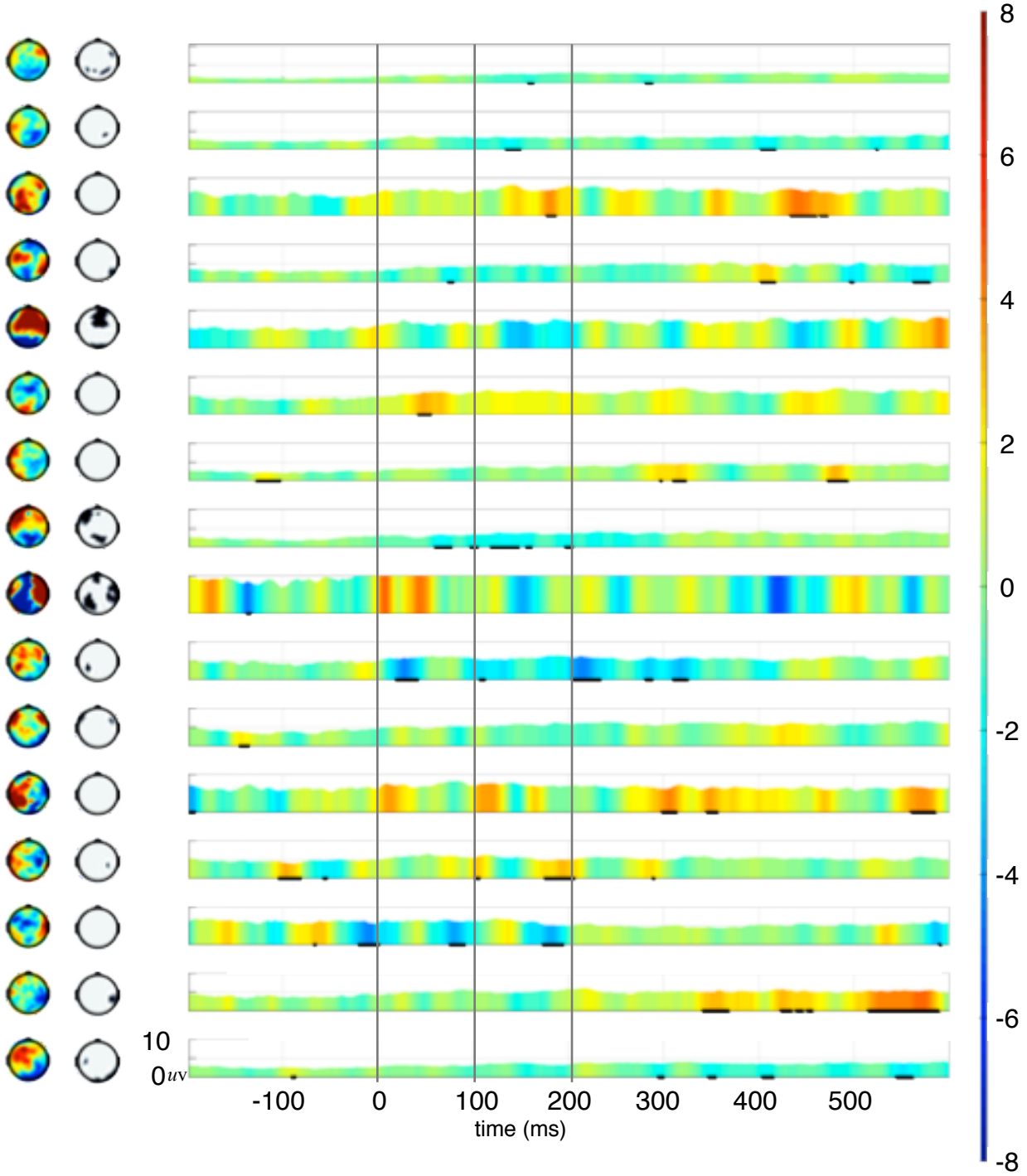

Figure 15. Single-subject results for the interaction. Horizontal colour bars represent mean differences between conditions at Oz. The margin of error (MOE) is shown on the Y axis. Topographic voltage differences and *p* values (<.05, black) are displayed at 152ms.

Frontal positivity effects

Group-level results for AS-AO and MS-MO. A main effect of awareness at approximately 320 ms was observed when comparing same and opposite conditions at Oz (at both aligned and misaligned levels). Topographical maps at that time period reveal a widespread statistical increase for same versus opposite conditions in frontal and parietal channels (and a corresponding decrease in occipital locations). Measured at Fz, this effect extended temporally from about 230-500 ms at both aligned and misaligned levels. The latencies correspond to the timing of the P3 component. Relative to the earlier N170 effects at Oz, this later effect at Fz are sizable across time, space, and in terms of mean μV difference (see Figure 16). This was true for both aligned same versus aligned opposite ($M_{(390ms)}$ = 2.3; 95% CI = [1.95 2.9], p<.05) and misaligned same versus misaligned opposite ($M_{(325ms)}$ = 2.2; 95% CI = [1.6 2.9], p<.05). No other noteworthy effects or interactions among conditions were found at the group level in the typical P3 latency range (see Figures 17 and 18).

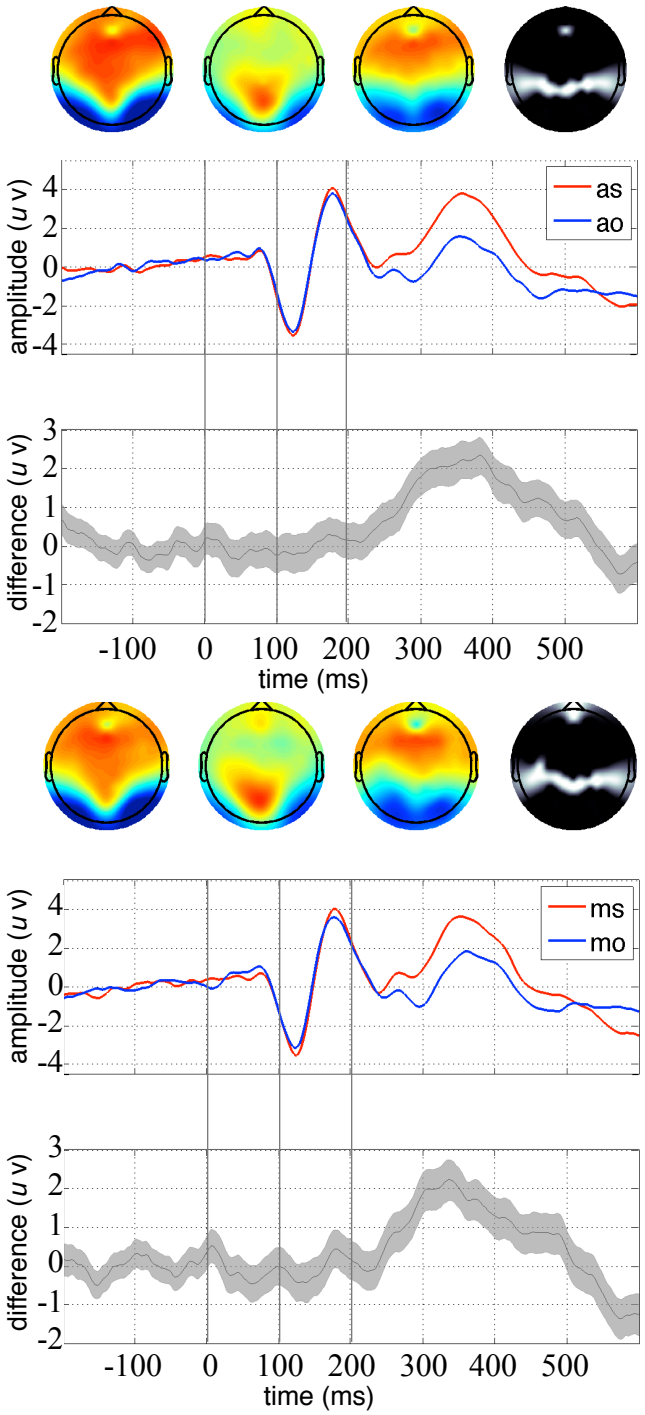

Figure 16. Top panel shows ERP waveforms measured at Fz comparing aligned same (as) and aligned opposite (ao) conditions. The corresponding 95% CI around the difference is shown in gray. Topographic voltage differences and *p* values (<.05, black) are displayed at 320ms. The bottom panel is identical but for the misaligned same (ms) and misaligned opposite (mo) comparison.

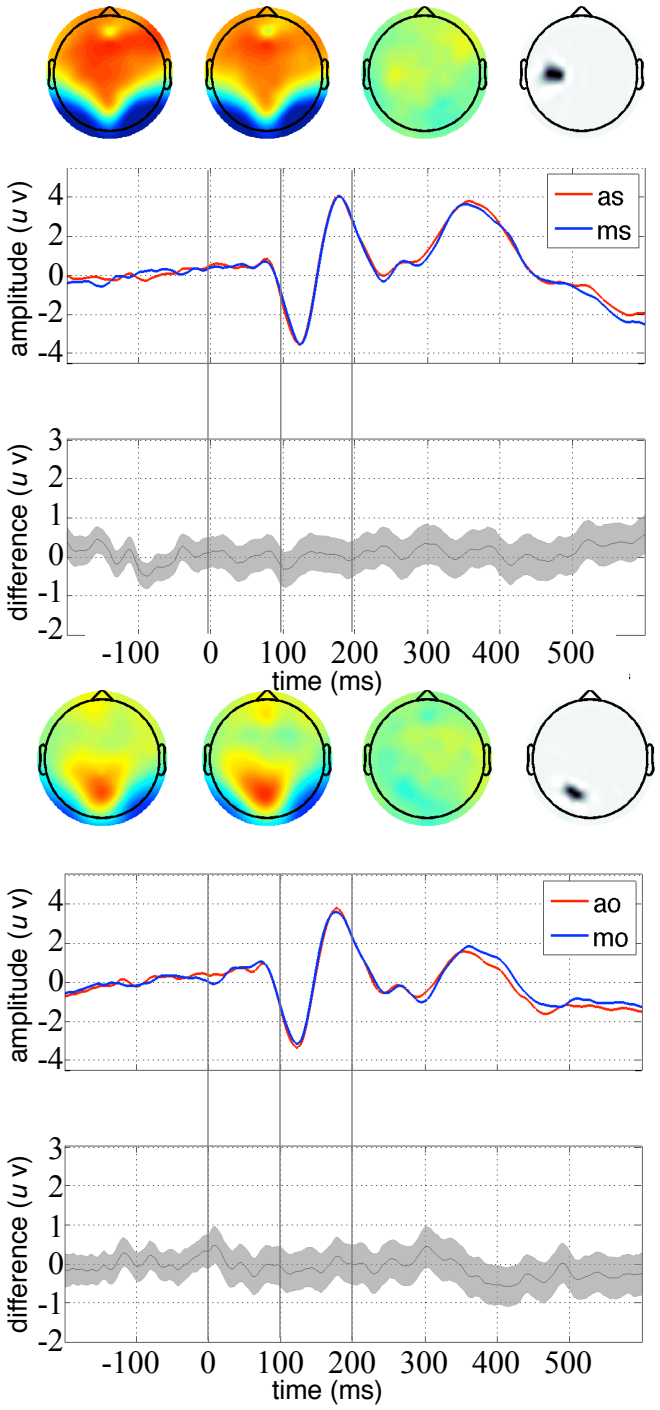

Figure 17. Top panel shows ERP waveforms measured at Fz comparing aligned same (as) and misaligned same (ms) conditions. The corresponding 95% CI around the difference is shown in gray. Topographic voltage differences and *p* values (<.05, black) are displayed at 320ms. The bottom panel is identical but for the aligned opposite (ao) and misaligned opposite (mo) comparison.

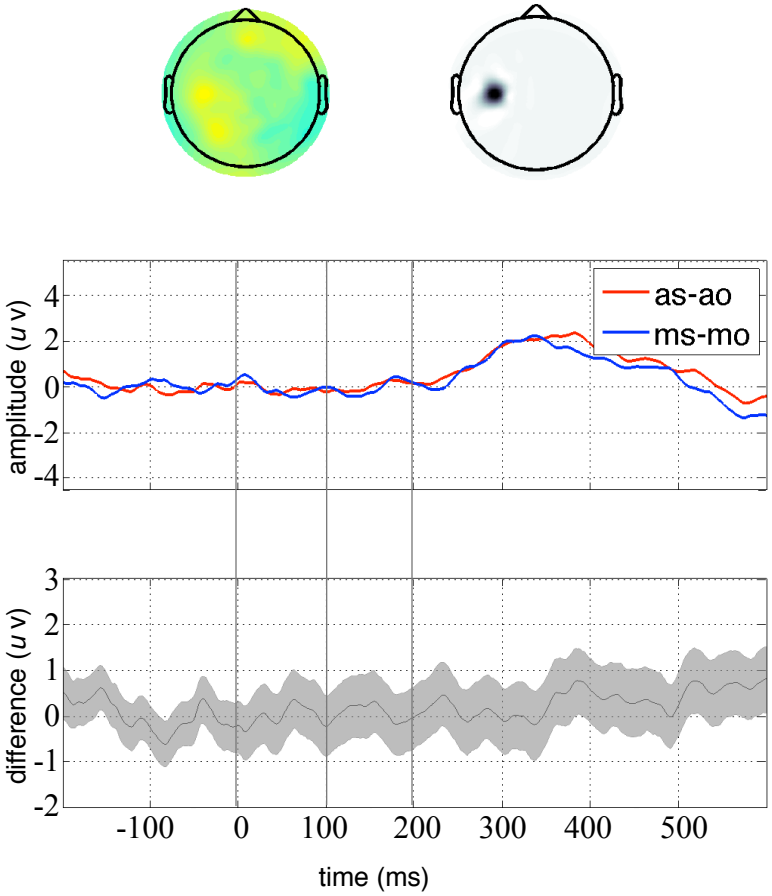

Figure 18. ERP waveforms measured at Fz for the interaction. The corresponding 95% CI around the difference is shown in gray. Topographic voltage differences and *p* values (<.05, black) are displayed at 320ms.

Single-subject results for AS-AO and MS-MO. Following up the main effect of awareness that was found at the group level, single-subject comparisons within same and opposite conditions (at both aligned and misaligned levels), reveal later effects that were highly consistent with the group findings, both temporally and spatially (see Figure 19 and 20). For example, 14 of 16 subjects showed statistical increases in the P3 time range (250 - 400 ms) in the aligned same versus aligned opposite comparison when measured at Fpz. A similar pattern was found for the misaligned same versus misaligned opposite comparison. No other noteworthy effects or interactions among conditions were found in the P3 latency range (250 - 400 ms) for the single-subject tests (see Figures 21, 22 and 23).

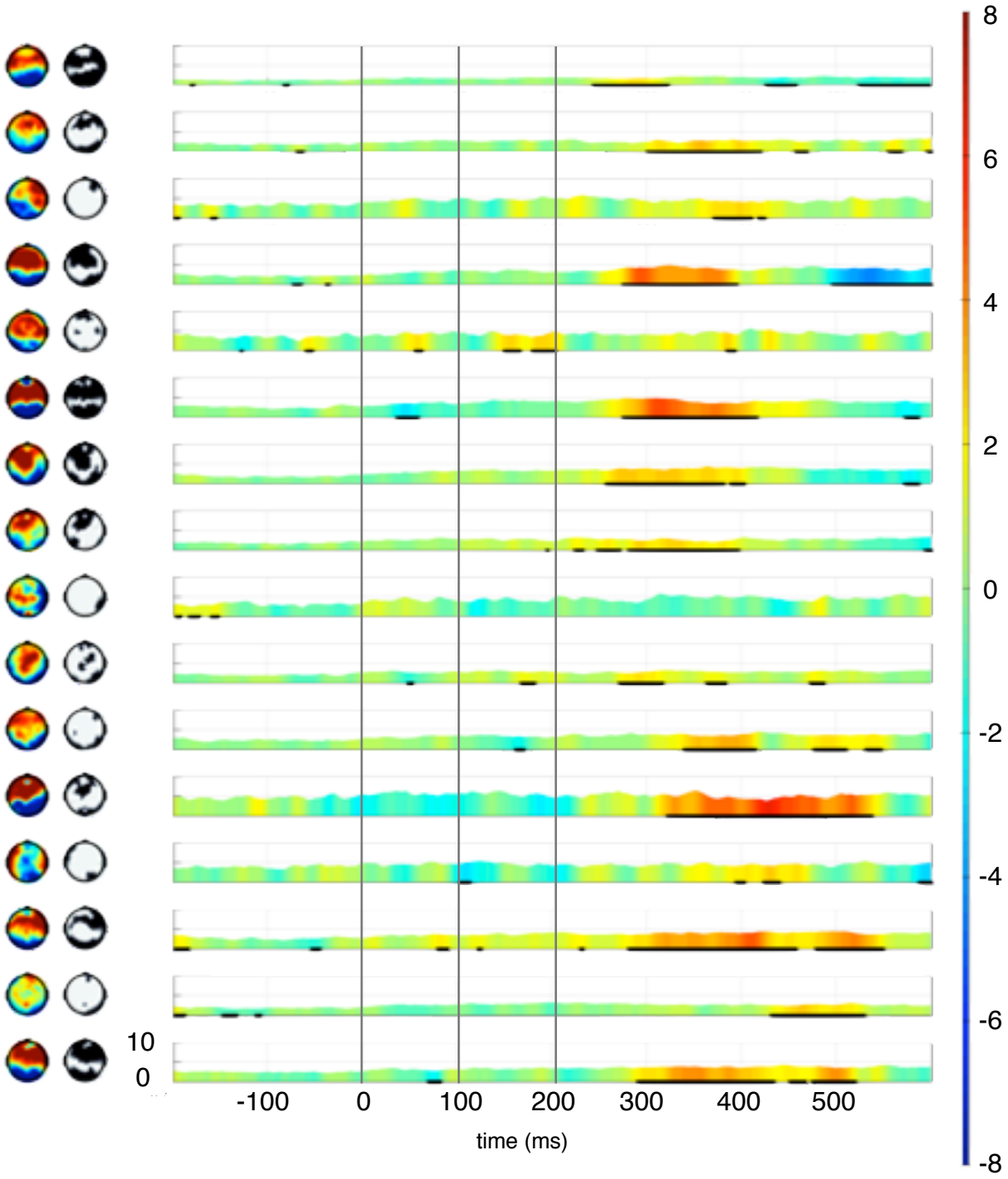

Figure 19. Single-subject results for aligned same versus aligned opposite. Horizontal colour bars represent mean differences between conditions at Fz. The margin of error (MOE) is shown on the Y axis (*u*v). Topographic voltage differences and *p* values (<.05, black) are displayed at 320ms.

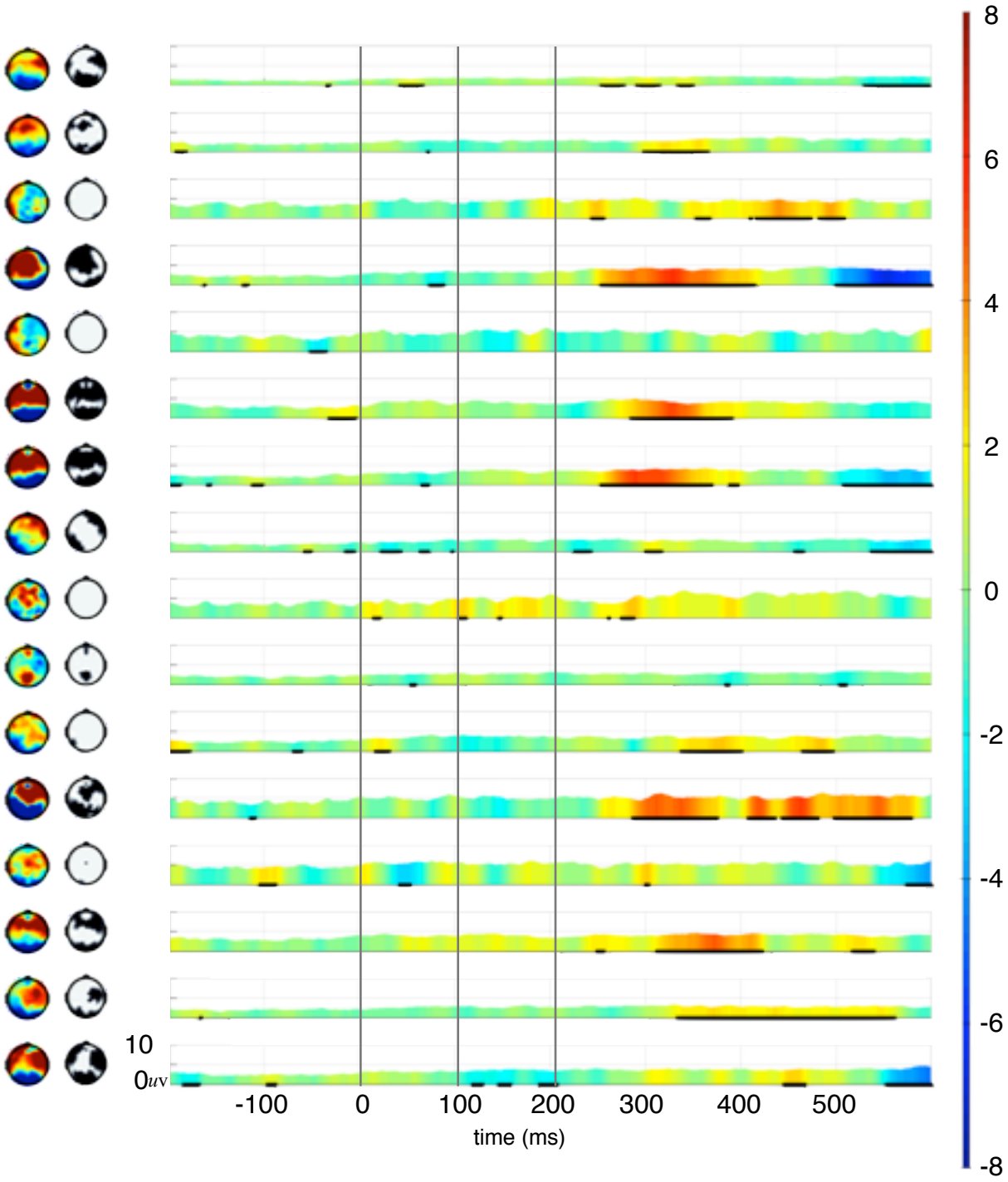

Figure 20. Single-subject results for misaligned same versus misaligned opposite. Horizontal colour bars represent mean differences between conditions at Fz. The margin of error (MOE) is shown on the Y axis. Topographic voltage differences and *p* values (<.05, black) are displayed at 320ms.

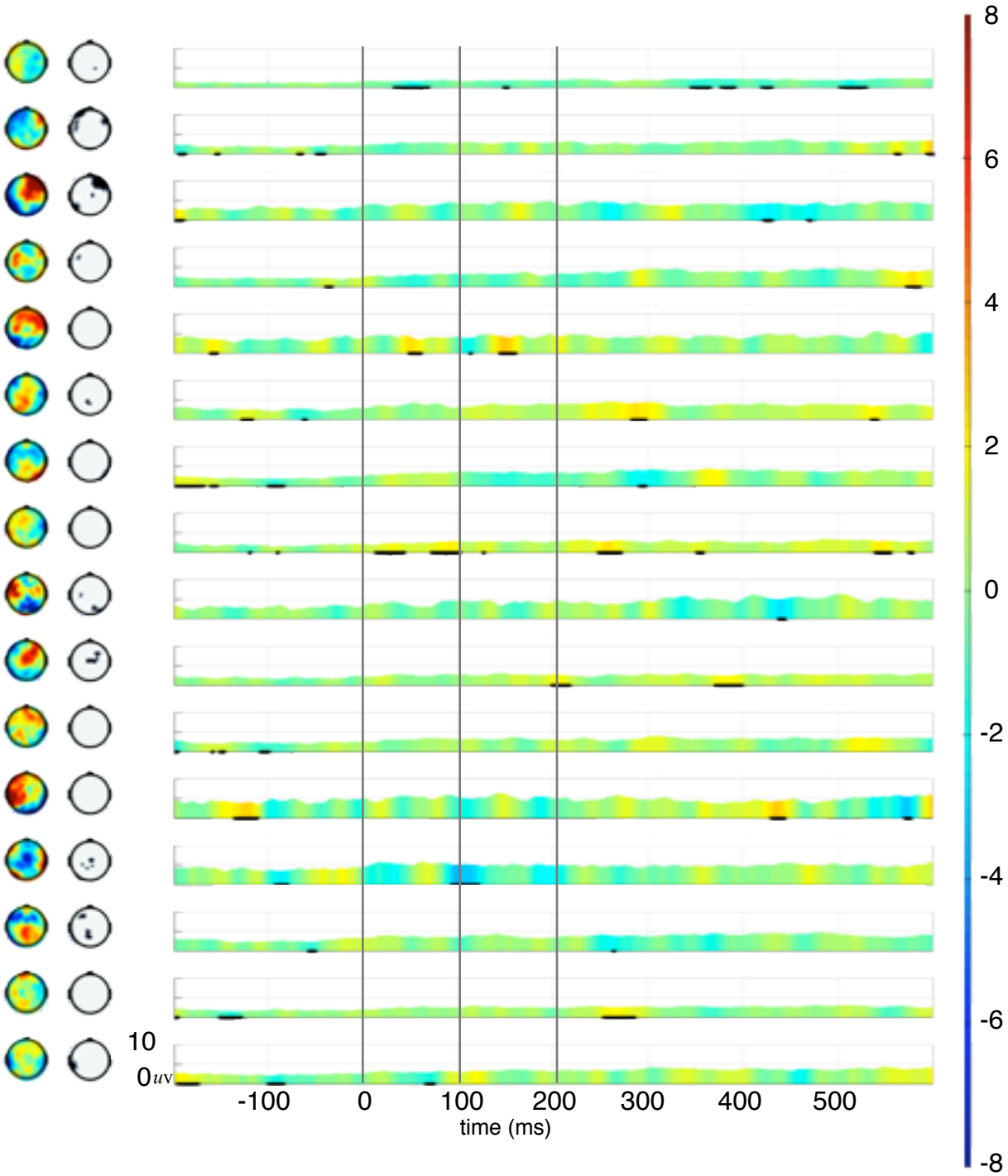

Figure 21. Single-subject results for aligned same versus misaligned same. Horizontal colour bars represent mean differences between conditions at Fz. The margin of error (MOE) is shown on the Y axis. Topographic voltage differences and *p* values (<.05, black) are displayed at 320ms.

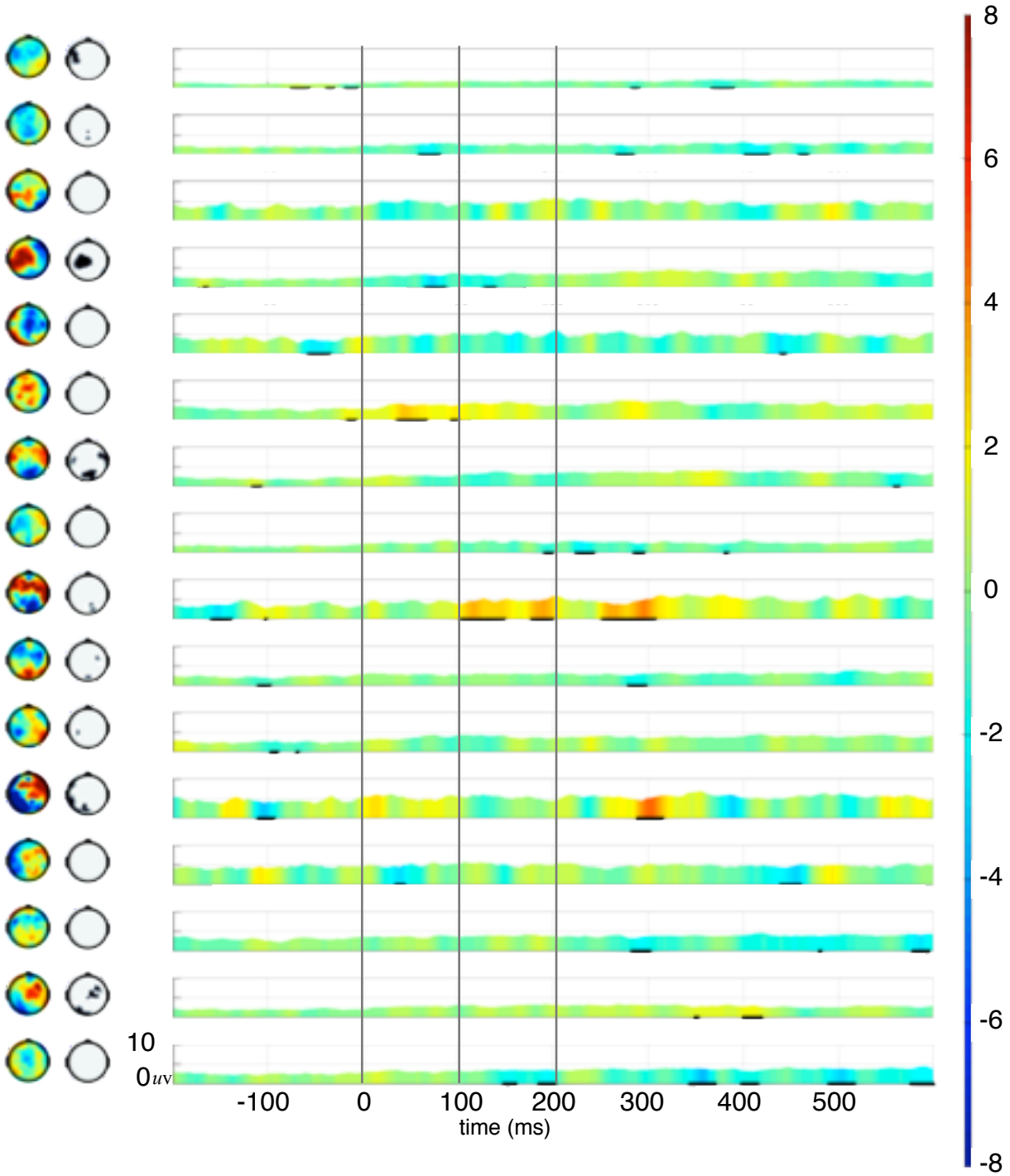

Figure 22. Single-subject results for aligned opposite versus misaligned opposite. Horizontal colour bars represent mean differences between conditions at Fz. The margin of error (MOE) is shown on the Y axis. Topographic voltage differences and *p* values (<.05, black) are displayed at 320ms.

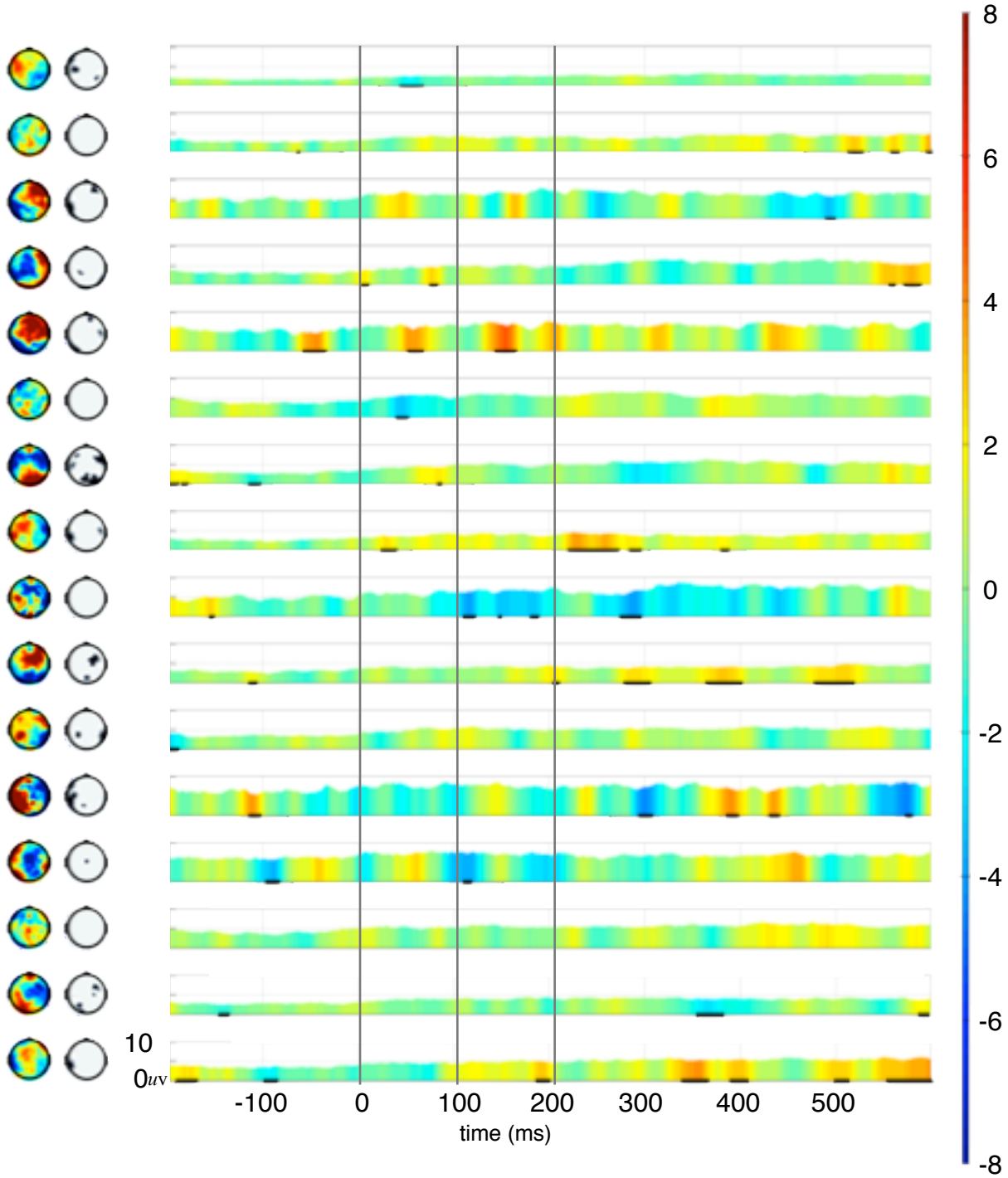

Figure 23. Single-subject results for the interaction. Horizontal colour bars represent mean differences between conditions at Fz. The margin of error (MOE) is shown on the Y axis. Topographic voltage differences and *p* values (<.05, black) are displayed at 320ms.

Discussion

Neural models of the processing of illusory contours diverge from one another in terms of their emphasis on bottom-up versus top-down constituents. The current study used dichoptic fusion to isolate electrocortical activity relating to the bottom-up processing of ICs. There were three hypotheses: (1) Kanizsa figures would elicit a larger N170 component than the misaligned control stimuli in general (i.e., when no dichoptic fusion is used). (2) The N170 effect would occur even when stimulus features defining the illusory figures are not made apparent to the participant (by means of dichoptic fusion). (3) The top-down model predicts an interaction such that the awareness factor will interact with the Kanizsa illusion and influence the N170. The first hypothesis is a validity check for the Kanizsa and misaligned control stimuli. The second hypothesis addresses whether or not there is evidence for bottom-up processing of ICs. The third hypothesis tests the interaction of top-down factors with the Kanizsa illusion which speaks to the tenability of a strong bottom-up model.

Implications of the N170 effect. The results indicate evidence for the IC effect at the time of the N170. I did not find evidence for IC effects at the P1 or P3 components as some others have found (Ikeda et al., 2011; Böttger et al., 2002). The time course and spatial spread of the IC effects found here are consistent with a number of studies showing negative-going ERP differences from about 150-180 ms that are spread across occipital sites (although previous studies often reported a more bilateral occipital effect, rather than the central occipital effect found here) (Murray et al., 2002; Murray et al., 2006; Pegna et al., 2002; Shpaner et al., 2011; Stanley & Rubin, 2003; Yoshino et al., 2006). Therefore the first hypothesis, a validity check for the stimuli was supported.

It must be mentioned however, that with a few exceptions, the group N170 effect reported here is not represented equally in the single-subject statistics. That is, a statistical effect in the group does not necessarily indicate a statistical effect in the individual subjects. It is probably true for most researchers that we hope, and maybe even assume, that group averages represent the bulk of the individuals. This is not the case in this particular study as is evident when observing the single-subject data. The inconsistencies between subjects may be due to cortical folding, skull thickness, or any physical characteristic that would affect electrocortical responses. Or perhaps the variability is due to other, more psychological reasons, such as differences in strategy, fatigue, or familiarity with the illusory stimuli (described below). In any event, this raises important questions concerning how we choose to approach multi-sensor data when studying ICs. For example, if cortical folding patterns vary sufficiently between subjects, neuronal responses of interest may be channeled to a variety of scalp locations. Thus, the traditional approach of analyzing the same sensor for the entire group is not appropriate, and may lead to missed effects. In the current study, statistical data are shown for all sensors and all subjects, and suggest that IC effects present themselves as negative deflections in occipital regions for most subjects; however, these are rarely statistically reliable decreases. This is not the first study to show inconsistencies at the single-subject level. Using MEG, Ohtani et al. (2002) showed an 80-150 ms IC effect in two of their four subjects. Furthermore, Mendola, Dale, Fischl, Liu, & Tootell, (1999) reported greater V1/V2 BOLD effects for ICs, but only at the group level. In fact, all of the sixteen subjects in that study failed to share the statistically reliable group effect. This was similar to Stanley and Rubin (2003) who found that only four of the eight

subjects in their study showed statistically greater BOLD activation for IC versus the control condition. Lesher (1995) comments,

> "Even with carefully defined measures, ratings of illusory contour strength are notorious for extravagant intersubject variations, particularly among naive subjects."

Indeed my subjects were naive to the illusion, as no attention was ever explicitly drawn to the ICs by the experimenter. Thus, based on the previous literature, the variability among individuals in the current experiment is to be expected to some degree.

No evidence of purely bottom-up processing of ICs was found by comparing the aligned opposite and misaligned opposite conditions. A null effect alone does not allow any definitive conclusion because absence of evidence is not evidence of absence (Sober, 2009). However, an interaction was found between awareness and the Kanizsa illusion. This provides support for top-down involvement during IC processing, thereby rendering a strong bottom-up model unlikely. According to these results, the N170 effect found in the literature (Murray, 2013), which is localized to the LOC, depends at least in part on the "knowing" of the Kanizsa illusion.

It is possible that the current paradigm has an inherent limitation and that the lack of a bottom-up effect is due to the degradation that the stimuli must undergo in order to be used in dichoptic fusion. The irony of this possibility does not escape me: It is possible that the very paradigm I used to isolate bottom-up effects may have prevented me from finding them. Specifically, the stimuli must be substantially altered from their optimal state by blurring and reducing the foreground/background contrast. Future studies exploring bottom-up effects should consider other paradigms that block top-down awareness but do not necessitate heavy alterations

of the stimulus features. In fact, alternative paradigms such as continuous flash suppression and attentional blink were considered prior to this experiment but dichoptic fusion seemed more appropriate for measuring ERPs given that these other methods involve flickering stimuli at a constant rate which induces steady-state potentials. Specifically, the associated electrocortical activity will oscillate at the frequency of the stimulus, or a multiple of it. Measuring steady-state potentials is a possibility for future studies; however, steady-state potentials may not directly map onto previous ERP findings given that, by definition, they would not produce typical P1-N1-P2 complexes, nor analogues to these. This is a practical issue to consider with respect to measurement and relating the findings to previous work.

Implications of the frontal positivity effect. Although it was not the primary focus of this thesis, the increased amplitude during the timing of the P3 to same versus opposite stimuli raises interesting thoughts on the neural timing and patterns of conscious awareness. The results here seem to suggest that the timing of conscious awareness of the stimulus begins around 300 ms and affects nearly every electrode. Furthermore, unlike the earlier N170 effects, the P3 effects are highly consistent across subjects, both in timing and topography. The consistency of activation in the single-subject effect is in line with previous studies (two of which used dichoptic fusion) claiming that the conscious awareness of the stimulus is associated with greater neural activation (Moutoussis & Zeki, 2002; Zeki & Ffytch, 1998; Schurger, et al., 2010). For example, Zeki and Ffytch (1998) studied patient GY who had sustained and injury to V1, rendering him hemianopic (blind in one visual field). When moving stimuli across GY's blind field, they noticed that GY's ability to detect the movement correlated with BOLD activity in area V5.

Electrophysiological data also demonstrate that neural activation correlates with the macaque's ability to detect change (Newsome, Britten, & Movshon, 1989). Specifically, using a random dot display, experimenters varied the percentage of dots that would move coherently along a continuum while simultaneously measuring activity in V5 (0% coherence means that dots would move randomly, and 100% coherence means that dots would all move together in the direction preferred by the neuron). They found that the monkey's ability to detect coherent motion of the dots positively correlated with the activity in V5. Therefore, psychophysical judgments were well-predicted by neuronal responses.

Other studies investigating the neural correlates of conscious awareness have reported similar effects to the ones described in the current study. For example, using a backwards masking paradigm to manipulate the conscious awareness of a target stimulus, Lamy, Salti, & Bar-Haim (2009) found larger and more spatially distributed P3 amplitudes on targets that subjects reported seeing compared to those they did not see. Effect sizes in their study are very similar to the current study as well, at approximately 2-3 *u*V increase for stimuli that were consciously perceived. The topographic spread of their effect, although maximal at posterior sites, is widely distributed and statistically significant across nearly the whole scalp, which is also what I observed in the current study. Several other studies, using a wide array of different paradigms, claim that the ERP correlate of conscious awareness exhibits itself as a large P3-like component that is widely distributed across the scalp (Babiloni, 2005; Del Cul, Baillet, & Dehaene, 2007; Fernan- dez-Duque, Grossi, Thornton, & Neville, 2003; Kranczioch, Debener, & Engel, 2003; Niedeggen, Wichmann, & Stoerig, 2001; Sergent, Baillet, & Dehaene, 2005; Turatto, Angrilli, Mazza, Umiltà, & Driver, 2002). Taken together, the aforementioned studies

provide some evidence which suggests that at the single-subject level as well as the group level, awareness of the stimulus is associated with increased neural activation. ERP studies, including the current one, show that this surge of neural activation exhibits itself as a widespread positivity at the scalp with a latency of approximately 300-500 ms.[9]

Conclusion

The current study presented the ERP timing and topographies statistically at the single-subject level, as it relates to IC processing, rather than relying solely on the examination of one or a few channels analyzed at a group level. At the group level, the Kanizsa illusion interacted with the awareness of the stimulus, leading to increased N170 amplitudes. This can be interpreted as evidence that the N170 effect found in the literature is dependent, at least partly, on the conscious awareness of the Kanizsa figures. Perhaps this top-down constituent is a result of feedback from the LOC to more primary visual areas as others have proposed, rather than a strictly feedforward process stemming from V1 and/or V2 areas; however, with the poor spatial resolution of EEG, this cannot be known for certain in the current study. Lastly, a product of the dichoptic fusion paradigm is the ability to look at the ERP correlates of the "knowing" of the stimulus. I found at both the group- and single-subject level that a widespread frontal positivity is the distinguishing factor for stimuli that are seen. A helpful future study could use dichoptic fusion, and perhaps other "top-down blocking" paradigms such as backwards masking or attentional blink to investigate potential bottom-up constituents of IC processing, as well as the ERP correlates of subjective awareness.

---

[9] Given that early evoked potentials may be affected by physical stimulus differences (Itier & Taylor, 2002; Johannes, Münte, Heinze, & Mangun, 1995; Regan, 1989; Rossion & Jacques, 2008; Willenbockel et al., 2010), and we did not find any early ERP differences (from 80-180ms) when testing MS-MO at Oz, or MS-MO and AS-AO at Fz, it is likely that the late effects of awareness in the current study are not confounded with physical stimulus differences.

References

Babiloni, C. (2005). Visuo-spatial Consciousness and Parieto-occipital Areas: A High-resolution EEG Study. *Cerebral Cortex*, *16*(1), 37–46. http://doi.org/10.1093/cercor/bhi082

Bell, A., & Sejnowski, T. J. (1995). An information-maximization approach to blind separation and blind deconvolution. *Neural Computation*, *7*(6), 1129–59. Retrieved from http://www.ncbi.nlm.nih.gov/pubmed/7584893

Berkovits, I., Hancock, G. R., & Nevitt, J. (2000). Bootstrap Resampling Approaches for Repeated Measure Designs: Relative Robustness to Sphericity and Normality Violations. *Educational and Psychological Measurement*, *60*(6), 877–892. http://doi.org/10.1177/00131640021970961

Böttger, D., Herrmann, C. S., & von Cramon, D. Y. (2002). Amplitude differences of evoked alpha and gamma oscillations in two different age groups. *International Journal of Psychophysiology : Official Journal of the International Organization of Psychophysiology*, *45*(3), 245–51. Retrieved from http://www.ncbi.nlm.nih.gov/pubmed/12208531

Del Cul, A., Baillet, S., & Dehaene, S. (2007). Brain Dynamics Underlying the Nonlinear Threshold for Access to Consciousness. *PLoS Biology*, *5*(10), e260. http://doi.org/10.1371/journal.pbio.0050260

Delorme, A., & Makeig, S. (2004). EEGLAB: an open source toolbox for analysis of single-trial EEG dynamics including independent component analysis. *Journal of Neuroscience Methods*, *134*(1), 9–21. http://doi.org/10.1016/j.jneumeth.2003.10.009

Desjardins, J., & Segalowitz, S. (2013). Deconstructing the early visual electrocortical responses to face and house stimuli. *Journal of Vision*, *13*, 1–18. http://doi.org/10.1167/13.5.22.doi

Ehrenstein, W., & Ehrenstein., A. (1999). Psychophysical Methods. In U. Windhorst. & H. Johansson (Eds.), *Modern Techniques in Neuroscience Research* (1211-1241) . New York: Springer.

Eriksson, J., & Nyberg, L. (2009). Details of the construction of perception: a closer look at illusory contours. *Frontiers in neuroscience*, *3*, 18.

Erkelens, C. J., & Regan, D. (1986). Human ocular vergence movements induced by changing size and disparity. *The Journal of Physiology*, *379*, 145–169.

Felleman, D. J., & Van Essen, D. C. (1991). Distributed hierarchical processing in the primate cerebral cortex. *Cerebral Cortex (New York, N.Y. : 1991)*, *1*(1), 1–47. http://doi.org/10.1093/cercor/1.1.1

Ffytche, D. H., & Zeki, S. (1996). Brain activity related to the perception of illusory contours. *NeuroImage*, *3*(2), 104–8. http://doi.org/10.1006/nimg.1996.0012

Fernandez-Duque, D., Grossi, G., Thornton, I. M., & Neville, H. J. (2003). Representation of change: separate electrophysiological markers of attention, awareness, and implicit processing. *Journal of Cognitive Neuroscience*, *15*(4), 491–507. http://doi.org/10.1162/089892903321662895

Grill-Spector, K., Kourtzi, Z., Kanwisher, N. (2001). The lateral occipital complex and its role in object recognition. *Vision Research*, *41*, 1409-1422.

Groppe, D. M., Urbach, T. P., & Kutas, M. (2011). Mass univariate analysis of event-related brain potentials/fields I: A critical tutorial review. *Psychophysiology*, *48*(12), 1711–1725. http://doi.org/10.1111/j.1469-8986.2011.01273.x

Halgren, E., Mendola, J., Chong, C. D. ., & Dale, A. M. (2003). Cortical activation to illusory shapes as measured with magnetoencephalography. *NeuroImage*, *18*(4), 1001–1009. http://doi.org/10.1016/S1053-8119(03)00045-4

Herrmann, C. S., & Bosch, V. (2001). Gestalt perception modulates early visual processing. *Neuroreport*, *12*(5), 901–4. Retrieved from http://www.ncbi.nlm.nih.gov/pubmed/11303756

Heydt, R., & Peterhans, E. (1989). Mechanisms of contour perception in monkey visual cortex. I. Lines of pattern discontinuity. *The Journal of neuroscience*, *9*(5), 1731-1748.

Heydt, R., Peterhans, E., & Baumgartner, G. (1984). Illusory contours and cortical neuron responses. *Science*, *224*(4654), 1260-1262.

Hirsch, J., & DeLaPaz, R. (1995). Illusory contours activate specific regions in human visual cortex: evidence from functional magnetic resonance imaging. *Proceedings of the National Academy of Sciences of the United States of America*, *92*, 6469–6473. Retrieved from http://www.pnas.org/content/92/14/6469.short

Ikeda, C., Kirino, E., Inoue, R., & Arai, H. (2011). Event-related potential study of illusory contour perception in schizophrenia. *Neuropsychobiology*, *64*(4), 231-238.

Itier, R. J., & Taylor, M. J. (2002). Inversion and contrast polarity reversal affect both encoding and recognition processes of unfamiliar faces: a repetition study using ERPs. *NeuroImage*, *15*(2), 353–72. http://doi.org/10.1006/nimg.2001.0982

Johannes, S., Münte, T. F., Heinze, H. J., & Mangun, G. R. (1995). Luminance and spatial attention effects on early visual processing. *Cognitive Brain Research*, *2*(3), 189–205. Retrieved from http://www.ncbi.nlm.nih.gov/pubmed/7580401

Kanizsa, G. (1955). Margini Quasi-Percettivi in Campi con Stimolazione Omogenea. *Rivista Di Psicologia*, *49*, 7–30.

Kanizsa, G. (1975). The role of regularity in perceptual organization. In *Studies on Perception* edited by G. B. Flores d'Arcais (Milano, Martello), 48–66.

Keselman, H., & Wilcox, R. (2004). A Power Comparison Of Robust Test Statistics Based On Adaptive Estimators. *Journal of Modern Applied Statistical Methods*, *3*(1), 27–38. Retrieved from http://eprints.usm.my/3102/

Knebel, J.-F., & Murray, M. M. (2012). Towards a resolution of conflicting models of illusory contour processing in humans. *NeuroImage*, *59*(3), 2808–17. http://doi.org/10.1016/j.neuroimage.2011.09.031

Kranczioch, C., Debener, S., & Engel, A. K. (2003). Event-related potential correlates of the attentional blink phenomenon. *Cognitive Brain Research*, *17*(1), 177–187. http://doi.org/S0926641003000922

Lamy, D., Salti, M., & Bar-Haim, Y. (2009). Neural correlates of subjective awareness and unconscious processing: an ERP study. *Journal of Cognitive Neuroscience*, 21, 1435–1446. http://doi.org/10.1162/jocn.2009.21064

Lesher, G. W. (1995). Illusory contours: Toward a neurally based perceptual theory. *Psychonomic Bulletin & Review*, *2*(3), 279-321.

Maertens, M., Pollmann, S., Hanke, M., Mildner, T., & Möller, H. (2008). Retinotopic activation in response to subjective contours in primary visual cortex. *Frontiers in Human Neuroscience*, *2*(April), 2. http://doi.org/10.3389/neuro.09.002.2008

Malach, R., Levy, I., & Hasson, U. (2002). The topography of high-order human object areas. *Trends in Cognitive Sciences*, *6*(4), 176-184.

Mendola, J. D., Dale, a M., Fischl, B., Liu, a K., & Tootell, R. B. (1999). The representation of illusory and real contours in human cortical visual areas revealed by functional magnetic resonance imaging. *The Journal of Neuroscience*, *19*(19), 8560–72. Retrieved from http://www.ncbi.nlm.nih.gov/pubmed/10493756

Michel, C. M., Murray, M. M., Lantz, G., Gonzalez, S., Spinelli, L., & Grave de Peralta, R. (2004). EEG source imaging. *Clinical Neurophysiology : Official Journal of the International Federation of Clinical Neurophysiology*, *115*(10), 2195–222. http://doi.org/10.1016/j.clinph.2004.06.001

Montaser-Kouhsari, L., Landy, M. S., Heeger, D. J., & Larsson, J. (2007). Orientation-selective adaptation to illusory contours in human visual cortex. *The Journal of Neuroscience : The Official Journal of the Society for Neuroscience*, *27*(9), 2186–95. http://doi.org/10.1523/JNEUROSCI.4173-06.2007

Moutoussis, K., & Zeki, S. (2002). The relationship between cortical activation and perception investigated with invisible stimuli. *Proceedings of the National Academy of Sciences of the United States of America*, *99*(14), 9527–32. http://doi.org/10.1073/pnas.142305699

Murray, M. M., Foxe, D. M., Javitt, D. C., & Foxe, J. J. (2004). Setting boundaries: brain dynamics of modal and amodal illusory shape completion in humans. *The Journal of Neuroscience : The Official Journal of the Society for Neuroscience*, *24*(31), 6898–903. http://doi.org/10.1523/JNEUROSCI.1996-04.2004

Murray, M. M., & Herrmann, C. S. (2013). Illusory contours: a window onto the neurophysiology of constructing perception. *Trends in Cognitive Sciences*, *17*(9), 471–81. http://doi.org/10.1016/j.tics.2013.07.004

Murray, M. M., Imber, M. L., Javitt, D. C., & Foxe, J. J. (2006). Boundary completion is automatic and dissociable from shape discrimination. *The Journal of Neuroscience : The Official Journal of the Society for Neuroscience*, *26*(46), 12043–54. http://doi.org/10.1523/JNEUROSCI.3225-06.2006

Murray, M., Wylie, G., Higgins, B. A., Javitt, D. C., Schroeder, C. E., & Fox, J. J. (2002). The Spatiotemporal Dynamics of Illusory Contour Processing: Combined High-Density Electrical Mapping, Source Analysis, and Functional Magnetic Resonance Imaging. *The Journal of Neuroscience*, *22*(12), 5055–73. Retrieved from http://www.ncbi.nlm.nih.gov/pubmed/12077201

Newsome, W., Britten, K., & Movshon, J. A. (1989). Neuronal correlates of a perceptual decision. *Nature*, *342*, 52–54. http://doi.org/doi:10.1038/341052a0

Niedeggen, M., Wichmann, P., & Stoerig, P. (2001). Change blindness and time to consciousness. *The European Journal of Neuroscience*, *14*(10), 1719–1726. http://doi.org/10.1046/j.0953-816x.2001.01785.x

Ohtani, Y., Okamura, S., Shibasaki, T., Arakawa, A., Yoshida, Y., Toyama, K., & Ejima, Y. (2002). Magnetic responses of human visual cortex to illusory contours. Neuroscience letters, 321(3), 173-176.

Oruç, I., Krigolson, O., Dalrymple, K., Nagamatsu, L. S., Handy, T. C., & Barton, J. J. S. (2011). Bootstrap analysis of the single subject with event related potentials. *Cognitive Neuropsychology*, *28*(5), 322–337. http://doi.org/10.1080/02643294.2011.648176

Pegna, A. J., Khateb, A., Murray, M. M., Landis, T., & Michel, C. M. (2002). Neural processing of illusory and real contours revealed by high-density ERP mapping. *Neuroreport*, *13*(7), 965–8. Retrieved from http://www.ncbi.nlm.nih.gov/pubmed/12004200

Peterhans, E., & von der Heydt, R. (1989). Mechanisms of contour perception in monkey visual cortex. II. Contours bridging gaps. *The Journal of neuroscience*, *9*(5), 1749-1763.

Pritchard, W. S., & Warm, J. S. (1983). Attentional processing and the subjective contour illusion. *Journal of experimental psychology*, *112*(2), 145-75. Retrieved from http://www.ncbi.nlm.nih.gov/pubmed/6223970

Purves D, Augustine GJ, Fitzpatrick D, et al., Eds. (2001). *Neuroscience*. Sunderland (MA): Sinauer Associates.

Ramsden, B. M., Hung, C. P., & Roe, a W. (2001). Real and illusory contour processing in area V1 of the primate: a cortical balancing act. *Cerebral Cortex (New York, N.Y.)*, *11*(7), 648–65. Retrieved from http://www.ncbi.nlm.nih.gov/pubmed/11415967

Regan, D. (1989). Human brain electrophysiology: Evoked potentials and evoked magnetic fields in science and medicine. 1989. New York: Elsevier, 1913. Retrieved from http://

scholar.google.com/scholar? hl=en&btnG=Search&q=intitle:ELECTROPHYSIOLOGY +Evoked+Potentials+and+Evoke d+Magnetic+Fields+in+Science+and+Medicine#0

Rousselet, G. A., Husk, J. S., Bennett, P. J., & Sekuler, A. B. (2008). Time course and robustness of ERP object and face differences. *Journal of Vision*, *8*, 1–18. http://doi.org/10.1167/8.12.3.Introduction

Rossion, B., & Jacques, C. (2008). Does physical interstimulus variance account for early electrophysiological face sensitive responses in the human brain? Ten lessons on the N170. *NeuroImage*, *39*(4), 1959–79. http://doi.org/10.1016/j.neuroimage.2007.10.011

Schumann, F. (1900). Beitraege zur Analyse der Gesichtswahrnehmungen. Erste Abhandlung. Einige Beobachtungen ueber die Zusammenfassung von Gesichtseindruecken zu Einheiten. *Z. Psychol. Physiol. Sinnesorgane*, *23*, 1–32.

Schurger, A. (2009). A very inexpensive MRI-compatible method for dichoptic visual stimulation. *Journal of Neuroscience Methods*, *177*(1), 199–202. http://doi.org/10.1016/j.jneumeth.2008.09.028

Schurger, A., Pereira, F., Treisman, A., & Cohen, J. D. (2010). Reproducibility distinguishes conscious from nonconscious neural representations. *Science (New York, N.Y.)*, *327*(5961), 97–9. http://doi.org/10.1126/science.1180029

Seghier, M., Dojat, M., Delon-Martin, C., Rubin, C., Warnking, J., Segebarth, C., & Bullier, J. (2000). Moving illusory contours activate primary visual cortex: an fMRI study. *Cerebral Cortex*, *10*(7), 663-670.

Seghier, M. L., & Vuilleumier, P. (2006). Functional neuroimaging findings on the human perception of illusory contours. *Neuroscience and Biobehavioral Reviews*, *30*, 595–612.

Sergent, C., Baillet, S., & Dehaene, S. (2005). Timing of the brain events underlying access to consciousness during the attentional blink. *Nature Neuroscienc*e, *8*(10), 1391–1400. http://doi.org/10.1038/nn1549

Sheth, B. R., Sharma, J., Rao, S. C., & Sur, M. (1996). Orientation maps of subjective contours in visual cortex. *Science*, *274*(5295), 2110-2115.

Shpaner, M., Murray, M. M., & Foxe, J. J. (2011). Early processing in human LOC is highly responsive to illusory contours but not to salient regions, *30*(10), 2018–2028. http://doi.org/10.1111/j.1460-9568.2009.06981.x.Early

Siegfried, J. B., Tepas, D. I., Sperling, H. G., & Hiss, R. H. (1965). Evoked Brain Potential Correlates of Psychophysical Responses: Heterochromatic Flicker Photometry. *Science (New York, N.Y.)*, *149*(3681), 321–323. http://doi.org/10.1126/science.149.3681.321

Sober, E. (2009). Absence of evidence and evidence of absence: Evidential transitivity in connection with fossils, fishing, fine-tuning, and firing squads. *Philosophical Studies*, *143*(1), 63–90. http://doi.org/10.1007/s11098-008-9315-0

Stanley, D. A., & Rubin, N. (2003). fMRI activation in response to illusory contours and salient regions in the human lateral occipital complex. *Neuron*, *37*(2), 323-331.

Turatto, M., Angrilli, A., Mazza, V., Umiltà, C., & Driver, J. (2002). Looking without seeing the background change: Electrophysiological correlates of change detection versus change blindness. *Cognition*, *84*(1), 1–10. http://doi.org/10.1016/S0010-0277(02)00016-1

Wilcox, R., & Keselman, H. (2000). Repeated measures ANOVA: Some new results on comparing trimmed means and means. *British Journal of Mathematical and Statistical Psychology*, *53*, 69–82. Retrieved from http://onlinelibrary.wiley.com/doi/10.1348/000711000159187/abstract

Wilcox, R. R. (2010). *Fundamentals of Modern Statistical Methods: Substantially Improving Power and Accuracy*. Springer. Retrieved from http://books.google.ca/books/about/Fundamentals_of_Modern_Statistical_Metho.html?id=uUNGzhdxk0kC&pgis=1

Wilcox, R. R., & Keselman, H. J. (2003). Modern robust data analysis methods: measures of central tendency. *Psychological Methods*, *8*(3), 254–74. http://doi.org/10.1037/1082-989X.8.3.254

Willenbockel, V., Sadr, J., Fiset, D., Horne, G. O., Gosselin, F., & Tanaka, J. W. (2010). Controlling low-level image properties: the SHINE toolbox. *Behavior Research Methods*, *42*(3), 671–84. http://doi.org/10.3758/BRM.42.3.671

Yoshino, A., Kawamoto, M., Yoshida, T., Kobayashi, N., Shigemura, J., Takahashi, Y., & Nomura, S. (2006). Activation time course of responses to illusory contours and salient region: a high-density electrical mapping comparison. *Brain Research*, *1071*(1), 137–44. http://doi.org/10.1016/j.brainres.2005.11.089

Zeki, S., & Ffytche, D. H. (1998). The Riddoch syndrome: Insights into the neurobiology of conscious vision. *Brain*, *121*(1), 25–45. http://doi.org/10.1093/brain/121.1.25